DOE/PC/93206--11

SCIENTIFIC AND TECHNICAL REPORT ON

"Temperature Effects on Chemical Structure and Motion in Coal"

DE-FG22-93PC93206

Report No. 11

Gary E. Maciel

Department of Chemistry

Colorado State University

Fort Collins, CO 80523

June 30, 1996

^{1}H-^{1}H SPIN EXCHANGE IN COAL

11.1 Introduction

We have previously demonstrated that various types of time domain experiments based on ^{1}H CRAMPS detection can provide structural and dynamical details of coal over a very broad range of spatial and time scales. The spatial structural heterogeneity of coal can be probed indirectly by these time-domain experiments because of the existence of efficient ^{1}H-^{1}H spin-diffusion in coals. However, the kinds of indirect studies of the ^{1}H-^{1}H spin-diffusion process presented in earlier chapters usually provide only qualitative information on structural heterogeneity. The direct study of the ^{1}H-^{1}H spin-diffusion process could provide further details on the structural heterogeneity of coal.

Both 1D and 2D ^{1}H-^{1}H spin-exchange experiments have been successfully used to investigate the heterogeneity of polymers on the spatial scale from 10 to 2000 Å[1-12]. These techniques have been proven to be very powerful tools for estimation of domain sizes in polymer blends[12]. However, there have been very few publications devoted to the direct study of ^{1}H-^{1}H spin-exchange processes in coal[13,14]. This is perhaps partly due to the fact that the chemical structures of coal are much more complicated and heterogeneous than those of synthetic polymers.

Tekely et al.[9] used a modified Goldman-Shen pulse sequence[30] with indirect ^{13}C CP/MAS detection to study spin-diffusion between rigid and mobile protons in an untreated French coal sample[13]. This study showed some potential for utilizing ^{1}H-^{1}H spin-diffusion information in coal studies, although the simple 1D spin-exchange experiment employed did not give conclusive results on the complicated spin-diffusion process in coal. The indirect ^{13}CP/MAS detection used in their study is also a questionable feature. Although a short contact time of 100 μs was used in their study, we

have shown in this work that significant ^1H-^1H spin-diffusion occurs within 100 μs in untreated coal samples.

Barton et al.[14] applied experiments of the type used by Zdzes and Samulski with ^1H wide line detection to C_5D_5N-imbibled bituminous coal samples. They used a dipolar-dephasing time of 60 μs to select relatively mobile proton species in C_5D_5N-saturated coal and concluded that mobile protons can rapidly spin-exchange with rigid protons within 10 ms. According to our dipolar-dephasing studies on C_5D_5N-saturated coal (Chapter 4), up to four distinctively different dipolar-dephasing constants can be identified for protons in C_5D_5N-saturated coal. Although a dipolar-dephasing time of 60 μs can eliminate almost all of the fast Gaussian dephasing component, a significant fraction of quite rigid protons that show slow Gaussian dephasing behavior are still retained in the signal. The spin-exchange process observed by Barton et al.[14] may result only from exchange among relatively rigid proton species.

Spin-exchange measurements among protons of different chemical functionalities would be very useful for studying chemical structural heterogeneity in coal. ^1H wide line detection is certainly unable to supply such valuable information. Knowledge of the spin-exchange processes in coal has been very limited. Expanding our knowledge in this area should provide valuable insights into the structural heterogeneity of coal.

In this report, we describe the first 1D and 2D ^1H-^1H spin-exchange studies of coals based on ^1H CRAMPS detection. We have designed and implemented a new 2D spin-exchange pulse sequence, which is able to probe complicated spin-exchange pathways among protons with different mobilities and chemical shifts. We demonstrate that 1D and 2D ^1H-^1H spin-exchange experiments are very useful for studying extremely heterogeneous systems such as coals.

11.2 Theory

11.2.1 ^1H-^1H Spin-Exchange Process

Both ^1H-^1H spin-diffusion and ^1H-^1H chemical exchange can be probed by a ^1H-^1H spin-exchange experiment. We use the term "spin-exchange" here to represent both the effects of ^1H-^1H spin-diffusion and chemical exchange. Although both processes can facilitate ^1H-^1H magnetization transfer, the underline physical processes are totally different. Chemical exchange occurs between pairs of labile protons that are close together and are able to exchange their chemical environments (chemical shifts) via a chemical reaction or a conformation change. Efficient long-distance chemical exchange is also possible through a network of hydrogen bonding. In an untreated (original) coal, ^1H-^1H chemical exchange is unlikely to be a significant contributor to ^1H-^1H spin-exchange process. In pyridine-saturated coals, chemical exchange could be significant, but is unlikely to be the dominant process of spin-exchange. The rate of chemical exchange would usually increase by thermal activation, but spin-diffusion would usually slow down at high temperature due to enhanced efficiency in the averaging of dipolar-couplings.

DISCLAIMER

Variable temperature experiments should in principle be able to separate effects of spin-exchange from spin-diffusion.

Spin diffusion is expected to be the dominant ^{1}H-^{1}H spin exchange mechanism in rigid, proton-rich solids, like coals. In the following discussion, we focus on the spin diffusion process. Contrary to what is suggested by the term "diffusion", spin-diffusion can be a coherent, reversible process. It is driven by the homonuclear dipolar Hamiltonian[12,15,16]. For a pair of spin ½ nuclei, the secular term of the homonuclear dipolar Hamiltonian reads

$$H_D = \omega_D(3I_{1z}I_{2z} - \vec{I}_1 \bullet \vec{I}_2),$$
$$\text{where} \qquad \omega_D = -\frac{\mu_0}{4\pi}\gamma^2\hbar\frac{1}{2}\frac{3\cos^2\theta - 1}{r^3} \tag{11.1}$$

If we express H_D in terms of raising and lowing operators, we get:

$$H_D = \omega_D\left[2I_{1z}I_{2z} - \frac{1}{2}\left(I_1^+I_2^- + I_1^-I_2^+\right)\right] \tag{11.2}$$

The term $(I_1^+I_2^- + I_1^-I_2^+)$ is usually called the flip-flop term. The flip-flop transition of two dipolar-coupled spins is an energy-conserving process. Considering the case in which only one of two spins is initially polarized, or the initial density operator is given by $\rho(0) = I_{1Z}$, the time evolution of $\rho(0)$ under H_D is governed by the propagator $\exp(-iH_Dt)$. As $(I_{1Z}\, I_{2Z})$ and $(I_1^+I_2^- + I_1^-I_2^+)$ commute, we can simplify the propagator as follows:

$$\exp(-iH_Dt) = \exp[i\frac{\omega_D}{2}(I_1^+I_2^- + I_1^-I_2^+)t]\exp[-i\omega_D(2I_{1z}I_{2z})t]. \tag{11.3}$$

Since $\exp(-i\omega_D 2I_{1Z}I_{2Z}t)$ commutes with I_{1Z}, the evolution of $\rho(0)$ will be affected only by the flip-flop term. The following expression for the evolution of $\rho(0)$ can thus be derived[12]:

$$\exp(-iH_Dt)I_{1z}\exp(iH_Dt) \rightarrow I_{1z}\frac{1}{2}(1+\cos\omega_Dt) + I_{2z}\frac{1}{2}(1-\cos\omega_Dt) + (I_{1y}I_{2x} - I_{1x}I_{2y})\sin\omega_Dt \tag{11.4}$$

This means that homonuclear polarization transfer $I_{1Z} \rightarrow I_{2Z}$ is realized via energy-conserving flip-flop processes.

Spin systems with spatially inhomogeneous z magnetization will evolve under the total dipolar Hamiltonian to minimize the z magnetization gradient through successive spin flip-flops. This coherent process is called spin-diffusion[15]. From equation (11.4), one sees that the transfer of z magnetization via spin flip-flops produces oscillations in a two-

sees that the transfer of z magnetization via spin flip-flops produces oscillations in a two-spin system. For spin system with large number of spins, the complicated coupling network cancels the oscillations and produce a diffusive behavior[12].

11.2.2 Spin-Diffusion Equation

For a large network of dipolar coupled spins, the effect of successive energy-conserving spin flip-flops can be described by a diffusion equation. For a radial spin diffusion process with an isotropic diffusion coefficient D, the diffusion equation reads[17,18]:

$$\frac{\partial\, m(r,t)}{\partial\, t} = D\frac{\partial^2 m(r,t)}{\partial\, r^2} \tag{11.5}$$

where m(r,t) represents magnetization at the radial position r and at the arbitrary moment of time t. If the diffusion process is spherical starting from a point source at $r = 0$, the solution of equation (11.5) is[17]

$$m(r,t) = \frac{m_0}{8(\pi\ Dt)^{3/2}} \exp(-\frac{r^2}{4Dt}) \tag{11.6}$$

where m_0 is the total magnetization.

The mean square distance $<r^2>$ that the magnetization has moved from the point source during the time t can be calculated from equation (11.6) as[18]:

$$\langle r^2 \rangle = \int_0^\infty r^2 \frac{m(r,t)}{m_0} 4\pi\ r^2 dr = 6Dt\,, \tag{11.7}$$

which permits us to use spin diffusion measurements to estimate finite domain sizes.

Of course, the spherical diffusion model is a simplified model of a real system. A more realistic model would include various morphologies, dimensionalities, and a distribution of diffusion time constants in the system. Many efforts have been devoted to develop various spin diffusion models for polymer systems[1,4,8,11]. As the structure of coal is much more complicated and heterogeneous than that of a synthetic polymer, at this stage, the information available is not enough for one to decide what kind of model is suitable for describing the spin diffusion process in coal quantitatively. Extensive experimental and theoretical work is needed to clarify this issue. Although the spherical diffusion model is simple, it does predict important spin-diffusion features which are in good agreement with much more sophisticated models[18,19]. In this work, we use this model for semi-quantitative estimation of structural heterogeneity in coal.

11.2.3 Spin-Diffusion Coefficients

In order to obtain information on domain size and morphology of a heterogeneous system, spin-diffusion coefficients must first be evaluated. If the morphology of a heterogeneous system is well defined, the spin-diffusion coefficient can be directly determined experimentally from spin-diffusion experiments on the system[8]. So far, there have been no direct experimental determinations of spin-diffusion coefficients on any coal samples.

Fortunately, spin-diffusion coefficients can be estimated indirectly from other experimental parameters. For a powder sample, the spin-diffusion coefficient D can be expressed in terms of local dipolar field as[1,20]

$$D = \sqrt{\frac{\pi}{60}} \langle d^2 \rangle B_L \tag{11.8}$$

where $<d^2>$ is the mean square distance between the nearest spins and B_L is the local magnetic field strength, due to local perturbations, expressed in the laboratory frame. If B_L is completely determined only by the contribution from dipolar interactions, B_L can be estimated as[21]

$$B_L^2 = \frac{5}{3} \overline{M}_2 \tag{11.9}$$

where $\overline{M}_2$ is the second moment of the NMR absorption line for a powder sample in a high magnetic field.

The second moment can be estimated directly from the dipolar-dephasing constant T_{dd}. For a Gaussian line shape[22],

$$\overline{M}_2 = \frac{1}{T_{dd}^2} \tag{11.10}$$

For a Lorentzian line shape, the integral diverges. However, truncation of the integral to the range $-\alpha < \omega < \alpha$, where α is a cut-off frequency, can give a pseudo-second moment[22]

$$\overline{M}_2 = \frac{2\alpha}{\pi T_{dd}} \equiv \frac{\beta}{\pi T_{dd}^2}, \tag{11.11}$$

where β is defined as $\beta \equiv 2\alpha T_{dd}$, which is a ratio of the frequency cut-off range 2α over $1/T_{dd}$. As a Lorentzian peak intensity drops below 1% of its maximum value when $\beta > 10$, we use $\beta = 10$ to estimate the $\overline{M}_2$ value of a Lorentzian line. Diffusion

coefficients for Gaussian and Lorentzian dephasing components can thus be estimated from dipolar-dephasing time constants via the following equations:

$$D_G = \frac{\sqrt{\pi}}{6}\frac{\langle d^2 \rangle}{T_{dd}} \qquad (11.12)$$

and

$$D_L = \frac{\sqrt{\beta}}{6}\frac{\langle d^2 \rangle}{T_{dd}}. \qquad (11.13)$$

As the exact molecular structure of coal is unknown, it is impossible to accurately estimate $<d^2>$. However, a semi-quantitative estimation of $<d^2>$ can be made from the known proton density of coal. Taking a typical value of hydrogen content of 5 wt% (dmmf: dry mineral matter free) and a density of 1.2 g/cm^3, a dmmf hydrogen volume percentage of about 6% (dmmf, cm^{-3}) in coal is obtained[23]. $\sqrt{<d^2>}$ can then be estimated as about 3 Å, assuming a cubic lattice of protons.

For the fast Gaussian dipolar-dephasing components in coal, a typical dephasing time constant is 10 μs. The spin-diffusion coefficient can then be estimated as 2.7×10^{-11} cm^2/s. For the slow Gaussian dephasing component with a dephasing time constant of 50 μs, the spin diffusion coefficient is about 5.3×10^{-12} cm^2/s according to Equation (11.12). In many organic polymer systems, D is on the order of 10^{-11} to 10^{-12} cm^2/s[12,18]. For example, D for a diblock copolymer of poly(styrene) and poly(methylmethacrylate)[8] was determined to be 8×10^{-12} cm^2/s; for polyethylene[4], D = 6.2×10^{-12} cm^2/s. So, the estimated spin-diffusion coefficients for coal is at least of the right order of magnitude. The inter-proton distance of 3 Å estimated above may be overestimated to some extent for rigid fast Gaussian dephasing components in coal, which could lead to an overestimation of the spin-diffusion coefficient for the fast Gaussian dephasing components.

11.2.4 Indirect Detection of Spin-Diffusion Process via Time-Domain Experiments

We have previously demonstrated that various time-domain experiments can provide detailed information on structural and dynamical heterogeneity of coal over a broad range of spatial dimensions. The spatial information obtained from those time-domain experiments relies on the ^{1}H-^{1}H spin-diffusion process in coal. As the proton density in coal is high and the ^{1}H-^{1}H dipolar interactions are strong, ^{1}H-^{1}H spin-diffusion in coal is fast. Such fast spin-diffusion processes tend to average out differences between dynamical behaviors of individual domains.

For a simple two-domain system, there are two limiting possibilities: the dynamical process of the system behaves as a single homogeneous system or as a physical mixture of two independent systems. In the first case, one can assume that the domains are small enough for spin-diffusion to average out the differences between the two domains. In the

latter case, the domains are too large for spin-diffusion to equalize the individual dynamical behaviors. If we assume that the intrinsic time constants of a certain dynamical process (e.g., spin-lattice relaxation, or dipolar dephasing) for domains A and B are T_A and T_B, the time constant of the system (T_s) that is effectively averaged by spin-diffusion would be

$$\frac{1}{T_s} = \frac{p_A}{T_A} + \frac{p_B}{T_B} \qquad (11.14)$$

where p_A and p_B are the relative fraction of protons in domains A and B, respectively.

If the domain sizes A and B are very large or spin-diffusion is very slow compared to T_A and T_B, the system will behave just like a mixture of two independent systems, and two separate time constants T_A and T_B are needed to describe the dynamical behavior of the system.

In the intermediate case in which the spin-diffusion rate is close to $1/T_A$ or $1/T_B$, the dynamical behavior of the two-domain system must still be described as two components, but the time constants of the two components are no longer the intrinsic time constants of the two separate domains (T_A and T_B). The spin-diffusion rate can be extracted quantitatively in this case from deviations of the two time constants relative to their intrinsic values (T_A and T_B values without spin diffusion between A and B)[24].

In any case, one can estimate the limit of the domain size L_D from the time constant T_S of a certain dynamical process in a specific domain as[18]:

$$L_D = \sqrt{\langle r^2 \rangle} = \sqrt{6DT_s} \qquad (11.15)$$

If the domain sizes are bigger than L_D, two different time constants T_A and T_B would be observed for the two domains. If the domain sizes are smaller than L_D, only one time constant, T_s, which is the average value of T_A and T_B, given in equation (11.14), would be observed.

For untreated coals, the ^1H-^1H dipolar dephasing time constant is on the order of 10 - 70 μs. If we use a spin-diffusion constant of 10×10^{-12} cm^2/s, a value that is typical of rigid organic solids, and a T_{dd} of 30 μs, we can estimate L_D as 4 Å. This means that dipolar-dephasing experiments can probe local structural heterogeneity of the system over only very short distances. Only domains that are intimately mixed on a molecule level will show a single dephasing time constant.

The rotating-frame ^1H spin-lattice relaxation time in untreated coals have been determined to be on the order of 1 - 15 ms. The dipolar interaction strength is scaled by ½ under a spin-lock condition. The spin-diffusion coefficient should correspondingly be scaled by ½. Using $D = 5 \times 10^{-12}$ cm^2/s and $T_{1\rho} = 10$ ms, we obtain $L_D(T_{1\rho}) \approx 55$ Å. In most cases, we have identified two $T_{1\rho}$ components in untreated coals. This suggests,

according to equation (11.15), that structural heterogeneity in coal also exists on a length scale of 50 Å.

The Zeeman spin-lattice relaxation time of an untreated coal is on the order of 60 ms to 300 ms. The limiting domain size L_D can be estimated from equation 11.15, using D $= 10 \times 10^{-12}$ cm^2/s and $T_1 = 200$ ms, as $L_D(T_1) \approx 350$ Å. We have also found that two relaxation components are needed to describe the proton spin-lattice relaxation of most coal samples. This implies that very large domains exist in coal.

The time-domain experiments outlined above clearly show that coal is an extremely heterogeneous material with structural, heterogeneity over a broad spatial dimension from 4 Å to 350 Å.

11.3 Experimental Methods and Details

11.3.1 1D Spin Exchange Experiment Based on CRAMPS

Figure 11.1 shows the general one-dimensional spin-exchange pulse sequence. It consists of three time periods: selection, mixing, and a detection period.

In the selection period, a gradient of spin temperature is created by utilization of different spectral and/or dynamical properties of different phases or domains of a system. For systems with well resolved chemical shifts from different phases, various chemical-shift selection schemes can be applied to select magnetization with certain chemical shift(s), thus creating a magnetization gradient between the phase(s) with the selected chemical shift(s) and the phase(s) with chemical shift(s) that are different from the selected value. In the presence of strong dipolar couplings, chemical shift selection can not be realized by simply irradiating a with long, soft pulse.

The DANTE pulse sequence is widely used for selective excitation in solid-state NMR[25-27]. However, to achieve selective excitation in a ^{1}H CRAMPS experiment, there is the added complication of combining DANTE-type pulse trains with the line-narrowing multiple-pulse sequences of CRAMPS. This combination has been implemented for the MREV-8 pulse sequence by alternating lengthened and shortened final pulses in the MREV-8 cycle[28]. If there are only a couple of resolved chemical shifts in a ^{1}H CRAMPS spectrum, a simplified scheme, termed the 'chemical-shift filter', which is based on chemical-shift differences, has been used for studying simple polymer blends[8,29]. As the ^{1}H CRAMPS resolution of bituminous coals is too poor to assure reliable chemical-shift selection, we did not use the chemical-shift selection approach in this work.

A commonly used strategy for creating a magnetization gradient relies on the heterogeneity of molecular motion in a system[30,4,11,29]. It includes selection schemes based on differences in the dipolar dephasing constant T_{dd}, the rotating-frame spin-lattice relaxation time $T_{1\rho}$, or the effective relaxation time (T_{1D}) under multiple-pulse irradiation. We have shown in previous chapters that coal is an extremely heterogeneous material at

We have shown in previous chapters that coal is an extremely heterogeneous material at the molecular level. Different behaviors in molecular dynamics have been observed for aliphatic protons and aromatic protons. Even for the same type of protons (either aliphatic or aromatic protons), distinctly different dipolar-dephasing constants T_{dd}, spin-lattice relaxation time T_1 and $T_{1\rho}$ have also been found in each individual coal sample. For example, four different dipolar-dephasing constants, spreading over four orders of magnitude, have been determined for aliphatic protons in pyridine-saturated premium coal 601. This extremely large motional heterogeneity in coal provides many possible schemes for magnetization selection.

In this work, we focused mainly on the selection scheme based on dipolar-dephasing constants, for the following reasons. First, coal components with different dipolar-dephasing constants in coal are related to molecular/macromolecular phases in coal. Measurements of spin exchange among components with different dipolar-dephasing constants should therefore provide details of coal structure in terms of the M/M model. Second, dipolar-dephasing constants are less affected by spin exchange than are spin-lattice relaxation times T_1 and $T_{1\rho}$, since dipolar-dephasing is much faster than spin-lattice relaxation processes in rigid solids, like coal. Thus, dipolar-dephasing constants reflect dynamical behaviors of individual small domains in coal. For an extremely heterogeneous system like coal, interpretations based on dipolar-dephasing processes should be more straightforward and simpler than those based on other relaxation processes.

The pulse sequence used in this work is an extension of the famous Goldman-Shen sequence[30], diagrammed in Figure 11.1b. With a dipolar dephasing period right after the first $\pi/2$ pulse, the Goldman-Shen experiment exploits the dipolar-dephasing time differences between rigid and mobile proton species to select magnetization of mobile species. The magnetization of mobile protons is then placed along the z direction by the second $\pi/2$ pulse. Spin exchange between rigid proton components and mobile proton components proceeds during the mixing period. The NMR signal is detected after the third $\pi/2$ pulse. Diffusion of magnetization from the mobile protons to the rigid protons is monitored with variable mixing period, and a diffusion constant can thus be determined.

The Goldman-Shen experiment was originally used for static samples, using the wide-line ^{1}H NMR detection technique. In this work, we implemented ^{1}H CRAMPS detection in the basic Goldman-Shen experiment. Although magic-angle spinning, an integral part of the CRAMPS technique, can slow down the spin-diffusion process, the spin-diffusion rate in rigid proton-rich solids should not be much affected by the modest MAS spinning speeds (around 1.6 kHz) used for ^{1}H CRAMPS detection[9]. This point is supported by dipolar-dephasing studies carried out earlier in this project. The dipolar-dephasing time constants obtained by ^{1}H CRAMPS detection in this work are very close to those measured by the ^{1}H wide-line technique on static samples[13]. This demonstrates that the modest MAS speed used in ^{1}H CRAMPS detection does not significantly lower the dipolar interaction strength, which determines spin diffusion rates.

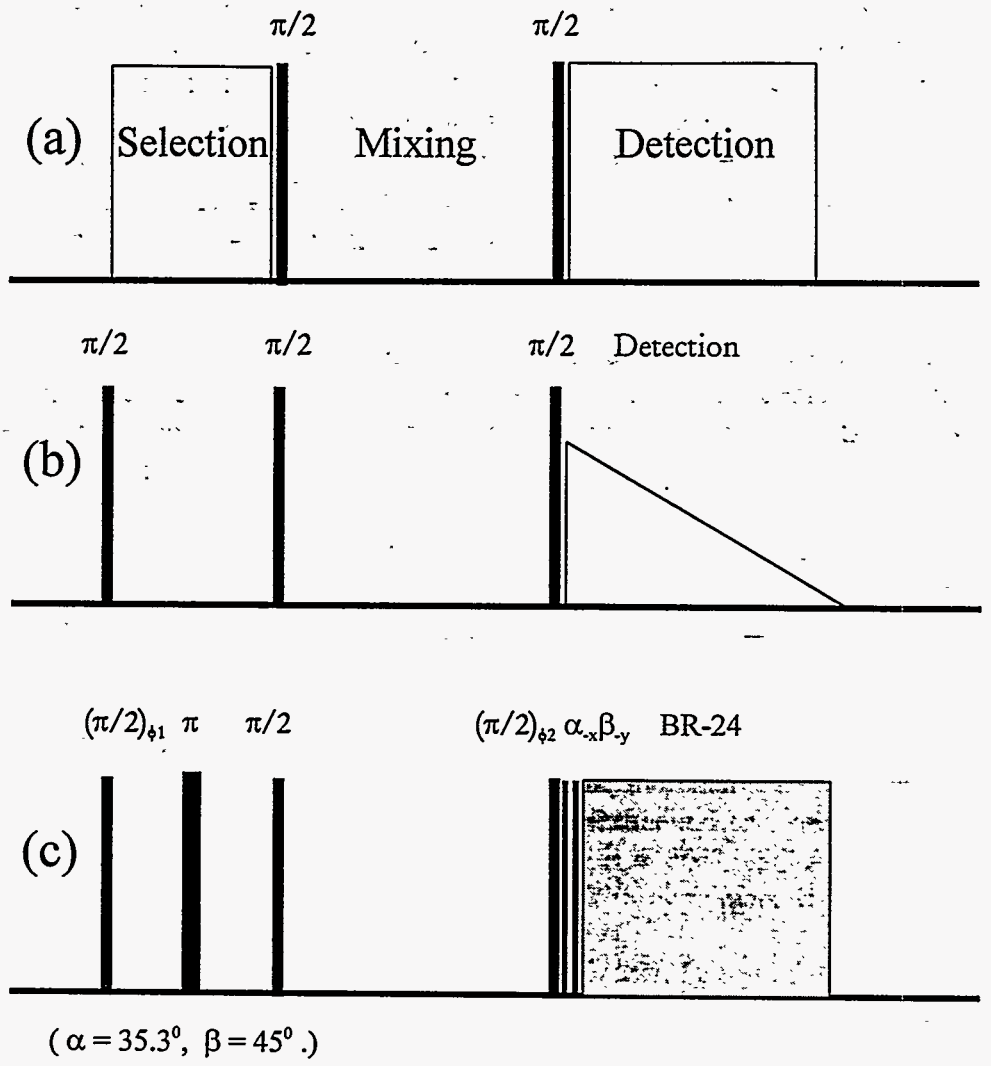

Scans	1	2	3	4
φ1	+x	-x	-x	+x
φ2	-x	-x	+x	+x
Receiver	-x	+x	+x	-x

Figure 11.1 Diagram of the 1D spin-exchange experiment. (a) A generic pulse sequence with three periods: selection, mixing, and detection. (b) Goldman-Shen experiment. (c) Improved 1D spin-exchange pulse sequence used in this work.

A modified Goldman-Shen experiment, with ^{1}H CRAMPS detection and a refocusing π pulse in the middle of dephasing period, has been used to study proton spin-exchange in silica gel and geminating seeds[31,32]. ^{1}H CRAMPS detection provides high resolution ^{1}H NMR spectra of solids. This makes it possible to detect spin-exchange among proton

species with different chemical shifts. The CRAMPS/Goldman-Shen approach has been improved in this work in two main respects. First, proper composite pulses are inserted prior to the ^{1}H CRAMPS detection period to maximize the detected signal intensity and minimize the spectral distortions caused by magnetization that is spin-locked along the effective field of a multiple pulse sequence; this is accomplished by aligning the magnetization perpendicular to the direction of the effective field prior to the multiple pulse cycles via the composite pulses. Second, a phase cycling procedure was implemented in order to: (i) eliminate baseline distortion caused by the residual magnetization that is still spin-locked along the effective field of a multiple-pulse sequence, (ii) compensate for spectral distortions caused by small misadjustment of pulse-widths and phases, (iii) reduce the distortion caused by multiple quantum coherence[3,33], and (iv) reduce the effect of spin-lattice relaxation during the mixing time[34].

11.3.2 A New 2D Spin-Exchange Experiment

We previously observed that proton spin-exchange in coals occurs on a time scale similar to that of ^{1}H dipolar-dephasing processes. Such spin-exchange and spin diffusion processes may be used to probe microscopic spatial heterogeneity due to either molecular mobility or chemical heterogeneity in coals. The one-dimensional spin-exchange experiments discussed above are very useful for monitoring the spin-exchange process among protons with different mobilities. However, spin-exchange among protons with different chemical shifts occurs at the same time as the exchange among protons of different mobilities in heterogeneous systems such as coal. As the spin-exchange pathways in coals are very complicated, a simple 1D spin-exchange experiment may not be suitable for probing the whole spin-exchange process.

The liquid-state two-dimensional (2D) exchange experiment (NOESY) is well known for its ability to monitor the complete exchange pathways of species with different chemical shifts[33]. An extension of the 2D exchange experiment to ^{1}H spin-exchange in rigid solids was made by Caravatti et al.[5]. Proton 2D spin diffusion experiments based on the MREV-8 line-narrowing sequence have been used successfully to study the miscibility and morphology of polymer blends[5]. This technique is very useful for identifying spin exchange pathways among spins with *different chemical shifts*. However, in coals, protons with quite different mobilities can have very similar chemical shifts, which are unresolved in ^{1}H CRAMPS spectra, as we have demonstrated in our earlier dipolar-dephasing experiments. Spin exchange processes among spins with overlapping chemical shifts but *different mobilities* cannot be investigated directly using the previously reported "standard" 2D spin exchange/diffusion experiments.

To address this problem, we designed a new 2D spin exchange pulse sequence. This sequence, shown in Figure 11.2, is able to probe the spin exchange pathways among spins with different chemical shifts and/or different mobilities. With the introduction of a dipolar-dephasing period in the preparation period, the new pulse sequence selects relatively mobile protons, discriminating against protons in rigid, proton-rich environments. Thus, gradients of Zeeman spin order among protons of different

mobilities, and possibly different chemical shifts, are established prior to the evolution and mixing periods. To encode chemical shift information into the t_1 dimension (evolution period), multiple-pulse cycles must be employed during that period. The multiple pulse train is also required during the evolution period for suppression of ^1H-^1H spin diffusion. During the mixing period, spins encoded in terms of both molecular mobility and chemical shift are allowed to transfer their Zeeman orders to other spins. ^1H CRAMPS detection provides chemical shift resolution in the second dimension of the resulting 2D exchange spectrum. With this new pulse sequence, spin exchange between rigid and mobile protons with unresolved chemical shifts can be detected from the broadening of peaks along the ω_2 axes of 2D exchange spectra; and spin exchange between protons with resolved chemical shifts can be readily identified from cross peaks.

To obtain the best CRAMPS resolution possible, we used BR-24 as the basis for the new 2D spin-exchange pulse sequence. To minimize baseline distortion and "pedestals" due to magnetization spin-locked along the direction of the effective field of the average Hamiltonian, composite pulses ($\alpha_{-x}\beta_{-y}$) are used in the pulse sequence to align magnetization perpendicular to this direction prior to the BR-24 cycles. Right after the evolution period, composite pulses ($\beta_y\phi_{-x}$) are also inserted before the mixing period to return the magnetization from the toggling frame[22] back to the xy plane of the rotating frame and bring the y component of magnetization to the direction of $\mathbf{B}_0$ (z). This composite pulse $\beta_y\phi_{-x}$ can be considered to be equivalent to $\beta_y\alpha_x(\pi/2)_{-x}$ with $\phi = \pi/2 - \alpha$. As the effective field of the average Hamiltonian of BR-24 is along the axis of $(\mathbf{e}_x - \mathbf{e}_y+\mathbf{e}_z)/\sqrt{3}$ in the rotating frame (where $\mathbf{e}_x$, $\mathbf{e}_y$ and $\mathbf{e}_z$ are unit vectors in this frame), the composite pulse used in this pulse sequence is just one of many possible composite pulses that could be used to serve the same purpose. In Figure 11.2b, we show another set of composite pulses for the same kind of 2D spin-exchange experiment, but using only single channel detection. This set of composite pulses is slightly simpler and easier to implement than those in Figure 11.2a. Details of the preparation pulse for a multiple-pulse sequence are discussed elsewhere. A phase cycling procedure has also been implemented for the same purposes as those discussed for 1D spin-exchange experiments. This phase cycling is indicated at the bottom of the pulse sequence in Figure 11.2.

For the best spectral resolution in a 2D experiment, the pure-absorption mode 2D spectrum is desired. For the pulse sequence with single channel detection, pure absorption 2D exchange spectra can easily be realized by setting the carrier frequency outside the spectral range and performing a real Fourier transformation with respect to t_1[12,33]. If quadrature detection in both dimensions is desired, which is unnecessary in most cases, the TPPI scheme can be easily adapted to the new pulse sequence to obtain pure absorption mode 2D spectra[33,35].

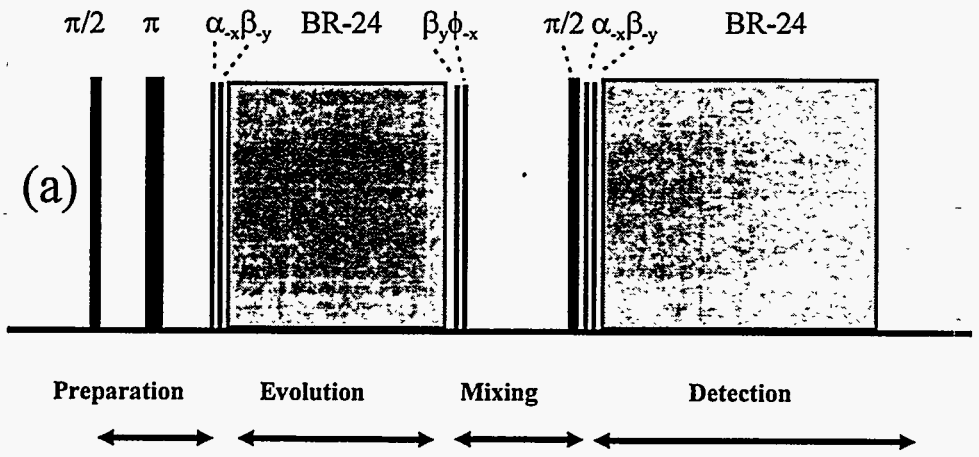

$\alpha = 35.3^0$, $\beta = 45^0$, $\phi = 54.7^0$.

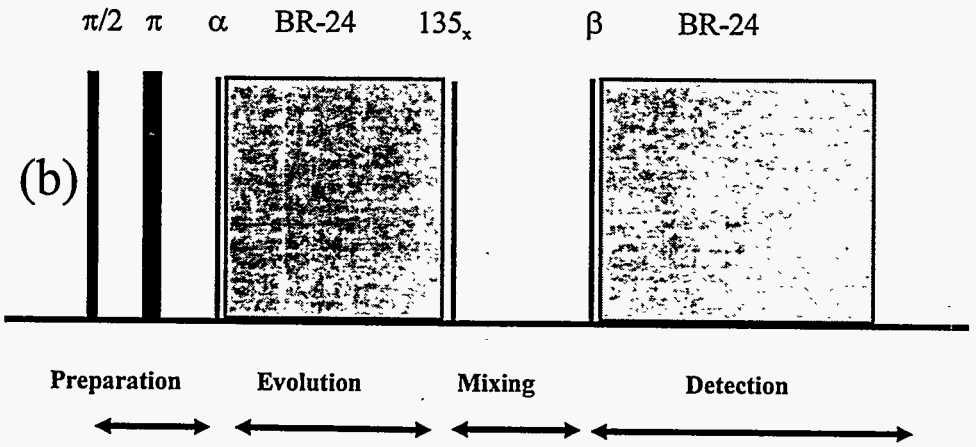

Phase Cycling				
Scan No.	1	2	3	4
α	135^0_{-x}	45^0_x	135^0_{-x}	45^0_x
β	45^0_x	45^0_x	135^0_{-x}	135^0_{-x}
Receiver	+x	-x	-x	+x

Figure 11.2 Diagrams of new pulse sequences for 2-D proton spin exchange experiments based on BR-24 CRAMPS. (a) The pulse sequence for quadrature detection. (b) The pulse sequence for single channel detection.

11.3.3 Experimental Details

^{1}H CRAMPS experiments were performed on a severely modified NT-200 NMR spectrometer operating at a proton Larmor frequency of 187 MHz[36]. A Chemagnetics VT CRAMPS probe was used in this work.

The coal samples used in this work are the same as those used in other experiments of this project. Details on sample preparation are documented elsewhere.

An appropriate dipolar-dephasing period was used in both 1D and 2D spin-exchange experiments to select components in coal with different mobilities. To select the slow Gaussian dephasing component from the fast dephasing component in untreated coal samples, a dipolar-dephasing period of 30 μs was used. As shown in Chapter 2, the dipolar-dephasing time constant of the fast Gaussian dephasing component is about 10 μs, while the dephasing time constant of the slow Gaussian dephasing component ranges from 30 to 70 μs. A dipolar-dephasing period of 30 μs achieves a 99% suppression of signals from the fast Gaussian dephasing component, and retains 40% - 93% of signals from the slow Gaussian dephasing component. For experiments on C_5D_5N-saturated coal samples, a dipolar dephasing period of 200 μs was used to select signals from Lorentzian dephasing components (dephasing time constants: 0.13 - 11 ms) and suppress signals from Gaussian dephasing components (dephasing time constants: 9 - 80 μs).

In the 2D spin-exchange experiments based on the new pulse sequences diagrammed in Figure 11.2, the increment of the evolution period (t_1) is the period of one BR-24 cycle, or 108 μs. Depending on the sample, either 64 or 128 increments were used in the evolution period, and 128 to 512 data points were acquired in the BR-24 detection period. We used single-channel detection with a carrier frequency on one side of the whole spectral region in all the experiments. The signal was averaged with 200 to 500 scans. The MAS rate was set as 1.6 ± 0.1 kHz. The recycle delay was 2 to 5 seconds. A complete 2D data set was processed according to standard procedures. To obtain pure absorption-mode 2D spectra, the time-domain data set was transformed to frequency domains by double real Fourier transformation.

11.4 Proton Spin Exchange in Untreated Premium Coals

11.4.1 Spin Exchange in Premium Coal 601

Figure 11.3 shows a stack plot of the ^{1}H CRAMPS spectra obtained in a 1D spin-exchange experiment on the untreated premium coal 601 at 25 ^{0}C. A dipolar-dephasing period of 30 μs was used to select the relatively mobile slow Gaussian dephasing component. According to the dipolar-dephasing time constants measured at 25 ^{0}C (Table 3.4), 5% of the signals from aliphatic protons and 13% of the signals from aromatic protons are retained after the dipolar-dephasing period. Comparing the ^{1}H CRAMPS

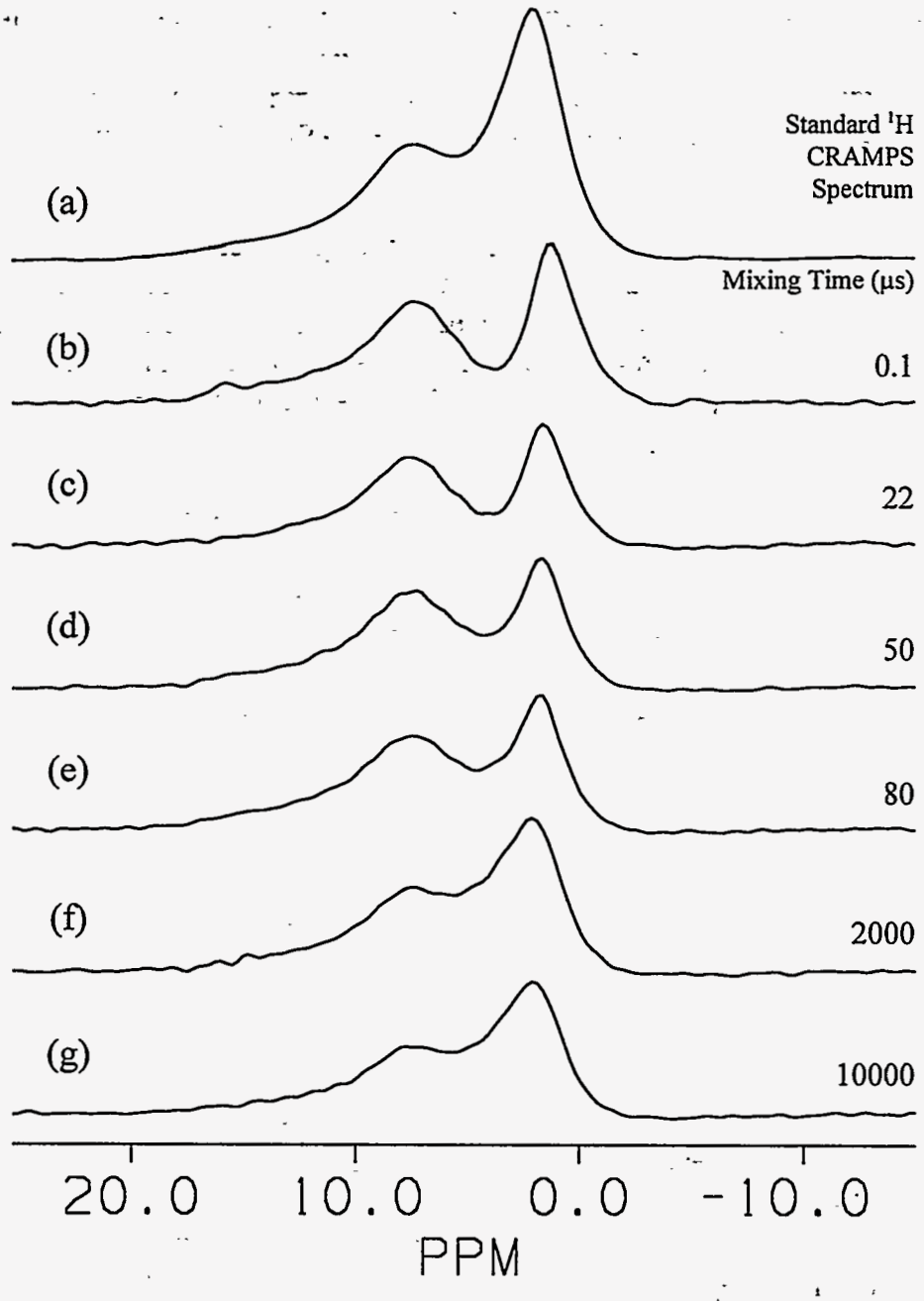

Figure 11.3 ^{1}H CRAMPS spectra of premium coal 601 obtained at 25 ^{0}C in a 1D spin-exchange experiment using the pulse sequence shown in Figure 11.1c. The mixing times were set as (b) 0.1 μs, (c) 22 μs, (d) 50 μs, (e) 80 μs, (f) 2 ms, and (g)10 ms. The dipolar dephasing period was 30 μs. The BR-24 pulse sequence with a cycle time of 108 μs and a 90^0 pulse width of 1.25 μs was used in the experiments. Each spectrum was acquired with 400 scans and a 3 s recycle delay. The MAS speed was 1.6 kHz. For comparison, a standard ^{1}H CRAMPS spectrum of premium coal 601 obtained at 25 ^{0}C is shown in (a).

spectrum with a dipolar-dephasing period of 30 μs and a mixing period of 0.1 μs (virtually no mixing period) (Figure 11.3b) with the original ^{1}H CRAMPS spectrum (Figure 11.3a), one can see a slight shift of the maximum of the aliphatic peak to higher shielding and a significant loss of signal intensity in the spectral region between 2 and 5 ppm. The change of peak shape in the aliphatic region suggests that non-methyl aliphatic protons dominate the rigid fast Gaussian dephasing component of aliphatic protons. As only one Gaussian dephasing component was identified for aromatic protons at 25 ^{0}C, the change of peak shape in the aromatic region during the 30 μs dipolar dephasing period is much less pronounced.

As shown in Figure 11.3, as a result of spin exchange that occurs during sufficiently long mixing times (e.g., >2 ms), the above-mentioned signal depletion in the region between 2 and 5 ppm recovers and the shape of the original ^{1}H CRAMPS spectrum returns. From the observed changes in peak shapes, one can clearly see that spin-exchange begins to show its significance at a mixing time of 50 μs, and essentially reaches an uniform spin temperature at a dephasing time of 2 ms. No significant additional change of peak shapes was observed with a dephasing time larger than 2 ms. We observe a slight decrease of total integrated spectral intensity (around 10%) with a dephasing time of 10 ms. This is due to the effect of spin-lattice relaxation during the mixing period. An intensity decrease of about 10% is expected at a mixing time of 10 ms based on the measured spin-lattice relaxation time at 25 ^{0}C. For untreated coal samples, spin exchange should be due mainly to spin diffusion, and chemical exchange is unlikely to be main mechanism of spin-exchange. The experimental 1D spin-exchange results clearly show that ^{1}H-^{1}H spin diffusion is very efficient in coal. Spin-diffusion in coal is significant on a time scale less than 100 μs. This is in agreement with the VT dipolar-dephasing studies carried out earlier in this project.

Comparing Figure 11.3a with Figures 11.3f and 11.3g, one can see that the peak shape of the standard ^{1}H CRAMPS spectrum (Fig. 11.3a) is not exactly the same as the spin-exchange spectra (Fig. 11.3f and 11.3g) obtained with sufficiently long mixing times. The intensity ratio of aliphatic to aromatic peaks in the standard ^{1}H CRAMPS spectrum is larger than those in spin-exchange spectra obtained with long mixing times of 2 ms and 10 ms. A mixing time of 10 ms corresponds to a spin diffusion distance of about 80 Å, according to equation (11.15), assuming a typical diffusion coefficient of $D = 5 \times 10^{-12}$ cm^2/s. If all the aliphatic structural units and aromatic structural units in coal are smaller than 80 Å, and they are randomly distributed in coal, the peak shape of the spin-exchange spectra obtained with a sufficiently long mixing time (≥ 10 ms) should be the same as the standard CRAMPS spectra of coal. The fact that we observed a difference in peak shapes implies that there exist large aliphatic-rich or/and aromatic-rich domains (larger than at least 80 Å) in premium coal 601. This is consistent with the spin-lattice relaxation (T_1) studies on premium coal 601, in which we concluded that aliphatic-rich domains larger than 350 Å exist in premium coal 601.

Aromatic protons can not effectively transfer their magnetization to the aliphatic protons in large aliphatic-rich domains. As 13% of the signals from aromatic protons and

only 5% of the signals from aliphatic protons are retained after the dipolar-dephasing period of 30 μs in the spin-exchange experiment, the intensity ratio of aliphatic to aromatic peaks in the spin-exchange spectra, even when obtained with a sufficiently long mixing period, would still be lower than that in the standard spectrum due to the existence of large aliphatic-rich domains. This is exactly what we observed in these spin-exchange experiments on premium coal 601. As we did not observe further significant changes of the peak shape of spin-exchange spectra obtained with mixing times longer than 2 ms, the aromatic units in the premium coal 601 must be surrounded by aliphatic structures with dimensions less than about 35 Å, which is the effective spin-diffusion distance corresponding to a mixing period of 2 ms. This result suggests that the aromatic structural units in premium coal 601 are not large. This finding is in agreement with the average aromatic cluster size derived from a ^{13}C CP/MAS study of HVB coals by Solum et al.[39].

If the spin-exchange pathway is well defined, the spin-exchange rate can in principle be extracted from a 1D spin-exchange experiment. However, spin-exchange pathways are very complicated in coal. From Figure 11.3, we can see that the magnetization from both mobile aliphatic and mobile aromatic protons are transferred to that of rigid non-methyl aliphatic protons. Quantifying such diffusion processes is difficult from a 1D spin-exchange experiment.

The detection of spin-exchange in a 1D spin-exchange experiment relies on changes in the shape and relative intensity of each peak. Spin-exchange processes among spins with overlapping chemical shifts but different mobilities can not be directly detected in a 1D spin-exchange experiment. A standard 2D spin-exchange experiment can not identify such exchange processes either. In order to elucidate the complete spin-exchange pathways among protons with different chemical shifts and/or different mobilities, we have designed a new 2D spin-exchange pulse sequence, which is described in Section 11.3.2. VT 2D spin-exchange experiments based on the new pulse sequence are discussed below.

Figure 11.4 presents contour plots of 2D spin-exchange spectra of premium coal 601 obtained at 25 ^0C with mixing periods of 0.1 μs, 50 μs, 500 μs and 5 ms. From Figure 11.4b (50 μs mixing time), one can clearly see a spread of spectral density along the ω_2 axis of the 2D exchange spectrum, and no appreciable cross peaks between aliphatic and aromatic protons. This suggests that spin-exchange among protons *within* either aliphatic structures or aromatic structures occurs very fast on the order of 50 μs. Assuming a typical diffusion coefficient of $D = 5 \times 10^{-12}$ cm^2/s, the spin diffusion distance corresponding to a 50 μs spin diffusion period can be estimated as 5 - 6 Å, according to equation (11.15). Thus, the 50 μs spin-exchange result suggests that an aliphatic (aromatic) proton in coal is surrounded most probably by other aliphatic (aromatic) protons within a sphere with a radius of 5 - 6 Å. The distribution of protons in coal can thus be visualized as a mixture of small clusters of aliphatic protons and small clusters of aromatic protons. This postulate can explain well the different dipolar-dephasing behaviors between aliphatic and aromatic protons. If these small aliphatic and aromatic proton clusters are distributed uniformly in the coal structure, one would not be able to observe large aliphatic-rich or aromatic-rich domains in coals. However, from spin-lattice

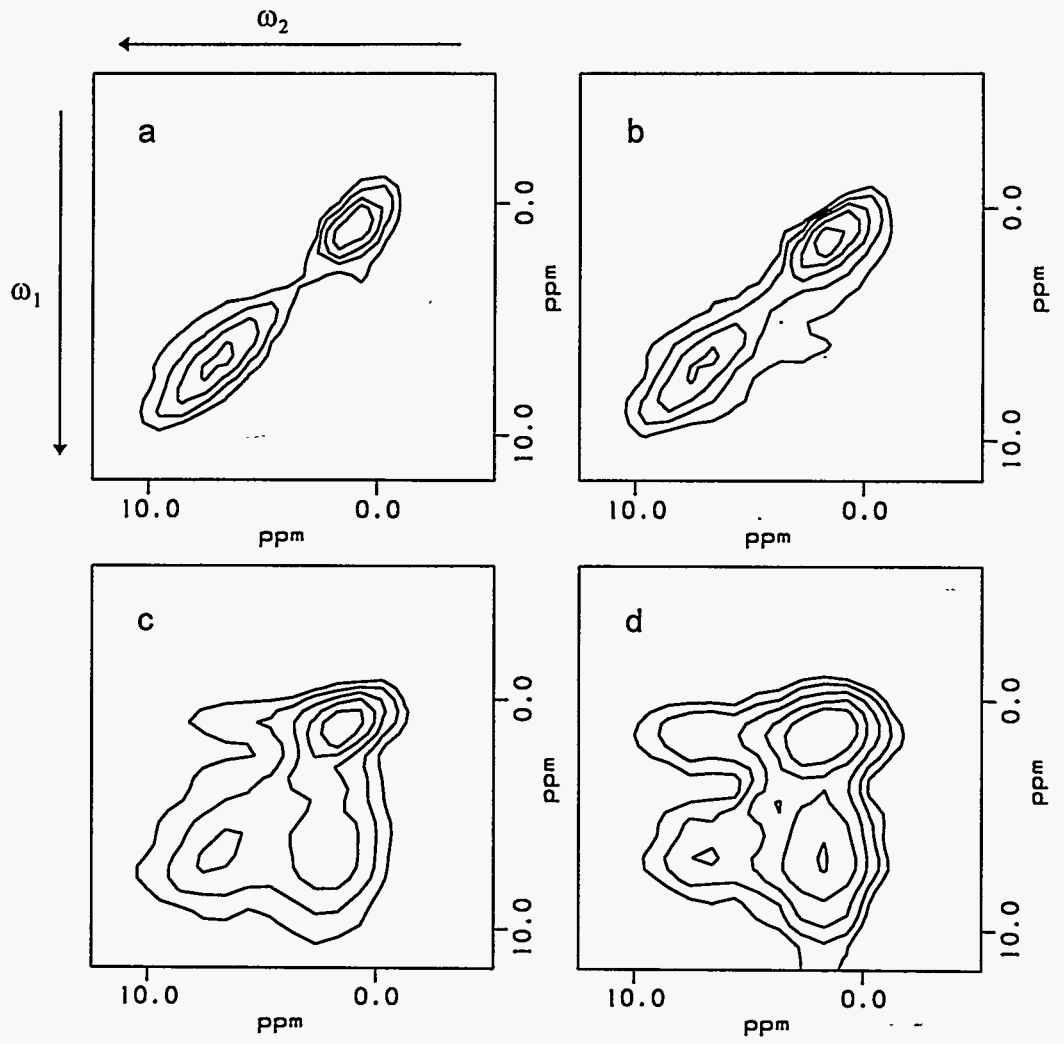

Figure 11.4 Contour plots of the pure absorption 2D ^{1}H-^{1}H spin-exchange spectra of premium coal 601 obtained at 25 ^{0}C with mixing times of (a) 0.1 μs, (b) 50 μs, (c) 500 μs, and (d) 5 ms. The pulse sequence used is that shown in Figure 11.2b, with a dephasing period of 30 μs. The increment of the evolution period was one BR-24 cycle, or 108 μs. The original data consisted of 64 256-point BR-24 spectra, each acquired with 400 scans and a 3 s recycle delay. The BR-24 pulse sequence was used with a cycle time of 108 μs and a 90^0 pulse width of 1.2 - 1.3 μs. The MAS speed was 1.6 kHz.

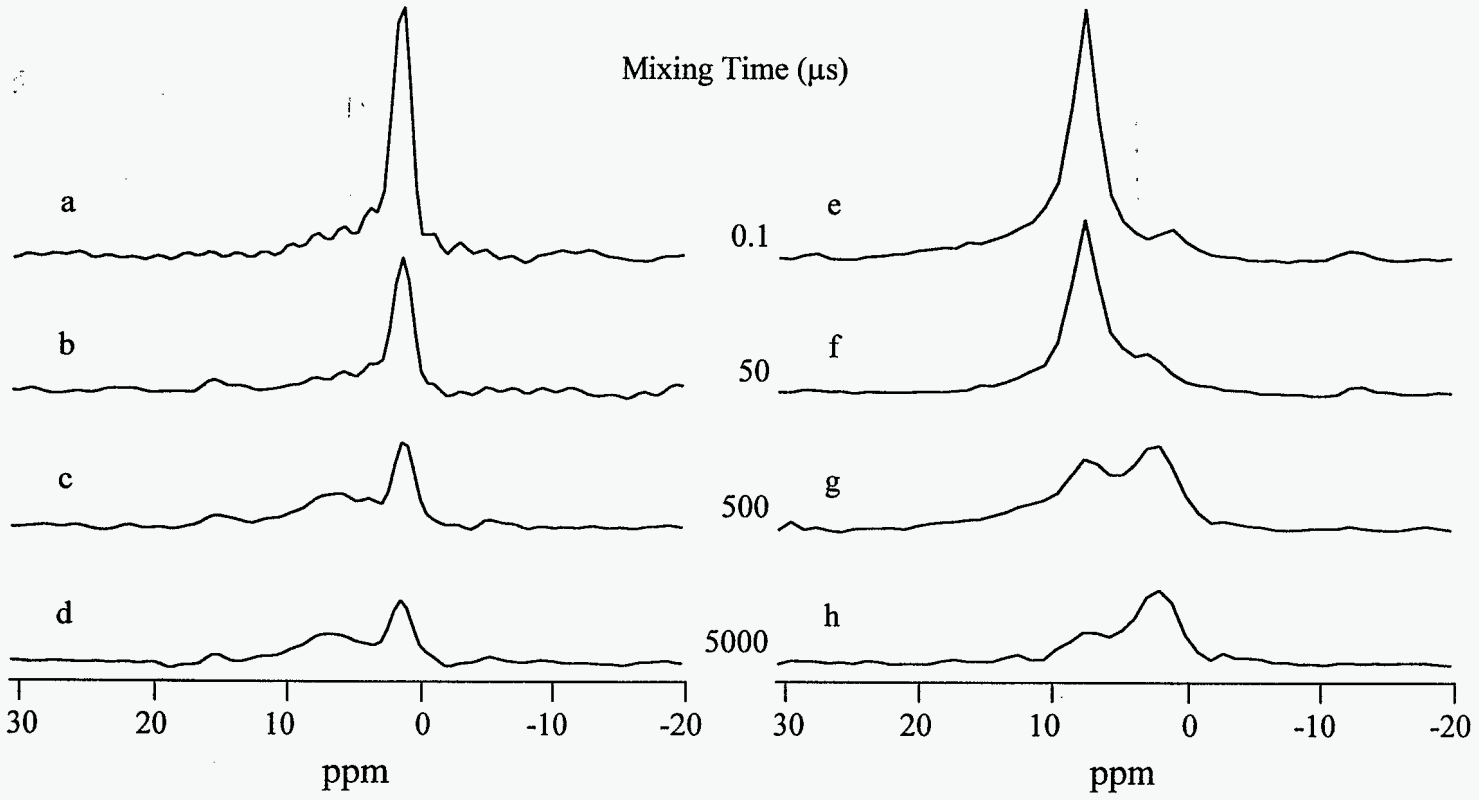

Figure 11.5 Slices cut from the 2D ^{1}H-^{1}H spin-exchange spectra of premium coal 601 shown in Figure 11.4. Slices cut along ω_1 at 1.0 ppm are shown in (a), (b), (c) and (d). Slices cut along ω_2 at 6.9 ppm are shown in (e), (f), (g) and (h). The corresponding mixing times used in the experiments are labeled by the side of each slice.

relaxation (T_1) studies on premium coal 601 carried out earlier, we concluded that large aliphatic-rich domains (on the order of 300 Å) exist in coal. Thus, the distribution of these small aliphatic and aromatic proton clusters (on the order of 5-6 Å) is not uniform within the coal structure.

With a mixing time of 500 μs (Figure 11.4c), cross peak intensity between aliphatic and aromatic protons is clearly seen, and aromatic and aliphatic diagonal peaks are severely broadened along both ω_2 and ω_1 axes. This means that extensive spin-exchange among protons with different chemical shifts and mobilities occur within 500 μs. According to equation (11.15), the spin-diffusion distance corresponding to a mixing time of 500 μs is estimated as about 17 Å. This suggests that a significant fraction of the aliphatic protons are located within a distance of 17 Å from aromatic protons.

As shown in the 2D spin-exchange spectra obtained from mixing times of 500 μs and 5 ms (Figures 11.4c and 11.4d), cross peak intensity between aliphatic protons and aromatic protons has continued to grow, because spin diffusion spreads over longer distances with increasing mixing time. A 5 ms mixing period corresponds to an effective spin-diffusion distance on the order of 55 Å. The 500 μs and 5 ms results suggest that aliphatic protons and aromatic protons separated by a distance more than 17 Å can exchange Zeeman order with a mixing period of 5 ms.

Some of the detailed spectral features of 2D exchange spectra are shown more clearly in slices cut parallel to either the ω_1 axis or the ω_2 axis. For example, the relative intensity of the lower-right cross peak between the aliphatic and aromatic protons can be compared with the intensity of the diagonal aliphatic peak in the slice cut parallel to the ω_1 axis; the relative intensity of the same cross peak to that of the aromatic diagonal peak can be seen in the slice cut parallel to the ω_2 axis. Figures 11.5a-d show slices cut parallel to the ω_1 axis at a chemical shift of 1.0 ppm. This set of slices illustrates intensity changes of the diagonal aliphatic peak and its cross peak in the aromatic region. There is some small residual spectral intensity in the aromatic region for slices corresponding to a mixing time of 0.1 μs (Figure 11.5a). This is certainly not a cross peak, and is due to the tail of the broad aromatic peak. When the mixing time is changed from 0.1 μs to 50 μs, the intensity of the aliphatic peak decreases appreciably due to broadening of the aliphatic peak along the ω_2-direction; there is no significant change of intensity in the aromatic region. This is consistent with the analysis based on 2D contour plots. Within a mixing period of 50 μs, spin exchange is limited within small aliphatic or aromatic domains, and there is no significant spin exchange between aliphatic protons and aromatic protons. With longer mixing periods (500 μs and 5 ms), spin diffusion between aliphatic and aromatic protons becomes significant. This is reflected in Figures 11.5c and 11.5d as a continual decrease of the diagonal aliphatic peak and a growth of the cross peak in the aromatic region as the mixing time is increased.

Figures 11.5e-h illustrate slices cut along the ω_2 axis at a chemical shift of 6.9 ppm. There is some small residual spectral intensity in the aliphatic region in the ^{1}H CRAMPS

spectrum obtained with a mixing time of 0.1 μs (Figure 11.5e). This is due to the tail of the broad aliphatic peak. With a mixing time of 50 μs, we can see the broadening of the diagonal aromatic peak at 6.7 ppm. As the mixing time is increased to 500 μs, the intensity of the cross peak at 1.0 ppm increases at the expense of the diagonal aromatic peak. The ^{1}H CRAMPS spectrum (Figure 11.5h) obtained with a mixing time of 5 ms is close to the "normal" ^{1}H CRAMPS spectrum of coal. This suggests that spin-exchange is close to complete.

Our previous dipolar-dephasing experiments suggest that the proton spin-exchange process is slowed down at higher temperature. A 2D spin-exchange experiment performed at high temperature should provide direct evidence on this assumption. Figure 11.6 shows contour plots of 2D spin-exchange spectra of premium coal 601 obtained at 180 ^{0}C, with a dipolar-dephasing period of 30 μs.

Based on the dipolar-dephasing constants measured at 180 ^{0}C, we can estimate that 37% of the signals from aromatic protons survive after the dephasing period (30 μs). Much higher fractions of proton signals are retained at 180 ^{0}C, because fractions of the slow Gaussian dephasing component are dramatically increased due to thermal activation. The fraction of aromatic signals remaining after 30 μs of dipolar dephasing is close to that of aliphatic protons at 180 ^{0}C, while the fraction of aromatic signals preserved is about 2.5 times that of aliphatic signals at 25 ^{0}C. This difference is clearly reflected in Figures 11.4 and 11.6. The relative intensity of the aliphatic peak is much higher at 180 ^{0}C than that at 25 ^{0}C.

The dependence of the 2D spin-exchange spectra on mixing time at 180 ^{0}C is similar to that at 25 ^{0}C. The spatial distribution of protons in coal derived from the above analysis of 2D spin-exchange spectra of coal at 25 ^{0}C are confirmed by the results obtained at 180 ^{0}C. As a result of a mixing time of 50 μs, expansion of the diagonal peak along ω_2 is much less pronounced than what we observed in the corresponding spectra obtained at 25 ^{0}C. This means that a higher temperature can retard the magnetization transfer from slow Gaussian dephasing components of aliphatic or aromatic protons to fast Gaussian dephasing components of the same structural type of protons. This explains why we can always identify two distinctively different dipolar-dephasing components at 180 ^{0}C, while sometimes only one dephasing component may be identified at 25 ^{0}C. Comparing the 2D spectrum acquired with a mixing time of 500 μs at 180 ^{0}C (Figure 11.6c) with that obtained at 25 ^{0}C (Figure 11.4c), we can see that the rate of spin-exchange between aliphatic and aromatic protons is also decreased at 180 ^{0}C. The 2D spectrum obtained with a mixing time of 5 ms at 180 ^{0}C (Figure 11.6d) is very similar to that obtained at 25 ^{0}C (Figure 11.4d). These results suggest that spin exchange among protons is almost complete within 5 ms at 180 ^{0}C, although the spin-exchange rate is significantly lower at 180 ^{0}C than at 25 ^{0}C.

These features seen in the 2D contour plots are also clear in slices cut along the ω_1 and ω_2 axes of the 2D spin-exchange spectra. Figures 11.7a-d show slices cut parallel to

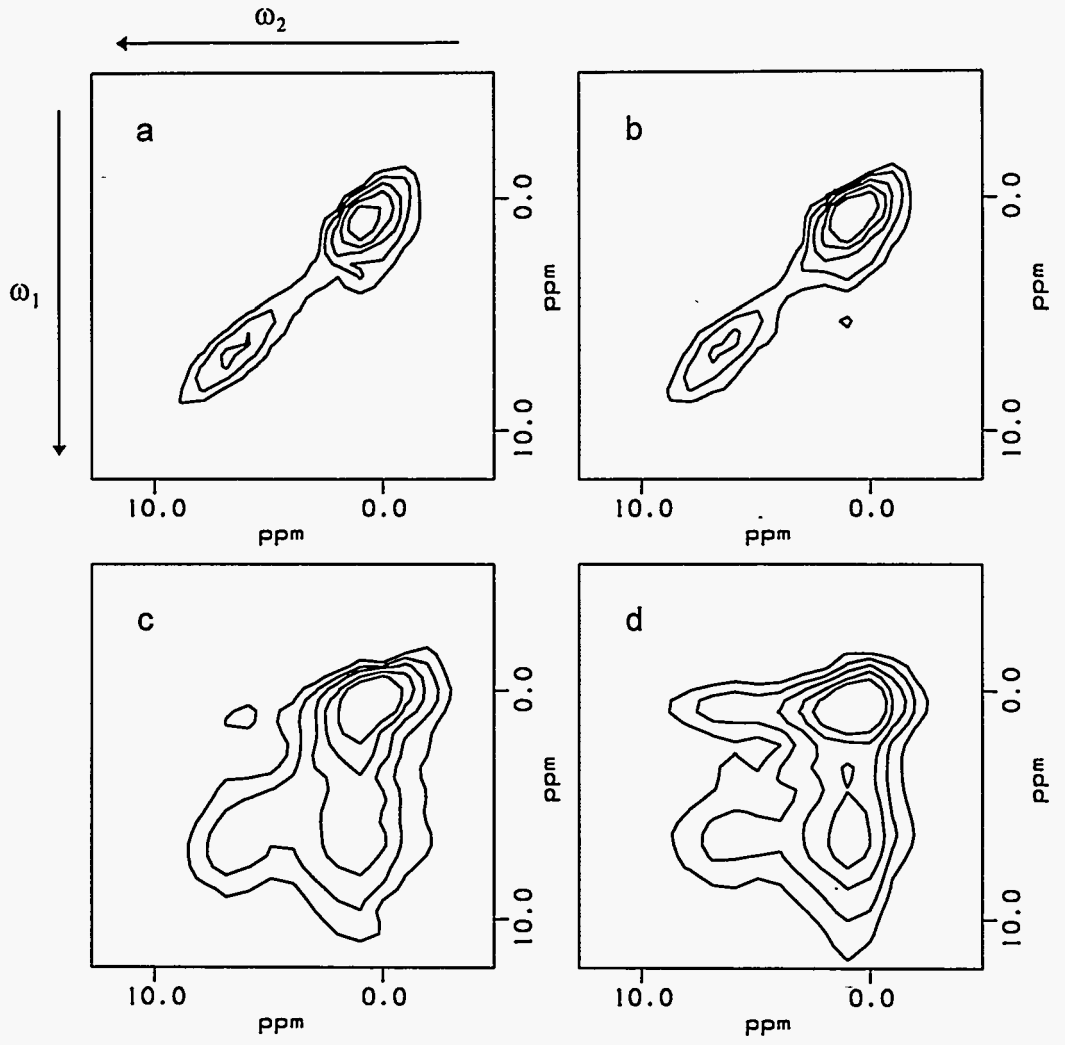

Figure 11.6 Contour plots of the pure absorption 2D ^{1}H-^{1}H spin-exchange spectra of premium coal 601 obtained at 180 ^{0}C with mixing times of (a) 0.1 μs, (b) 50 μs, (c) 500 μs, and (d) 5 ms. The pulse sequence is that shown in Figure 11.2b, with a dephasing period of 30 μs. The increment of the evolution period was one BR-24 cycle, or 108 μs. The original data consisted of 64 256-point BR-24 spectra, each acquired with 400 scans and a 3 s recycle delay. The BR-24 pulse sequence was used with a cycle time of 108 μs and a 90^0 pulse width of 1.2 - 1.3 μs. The MAS speed was 1.6 kHz.

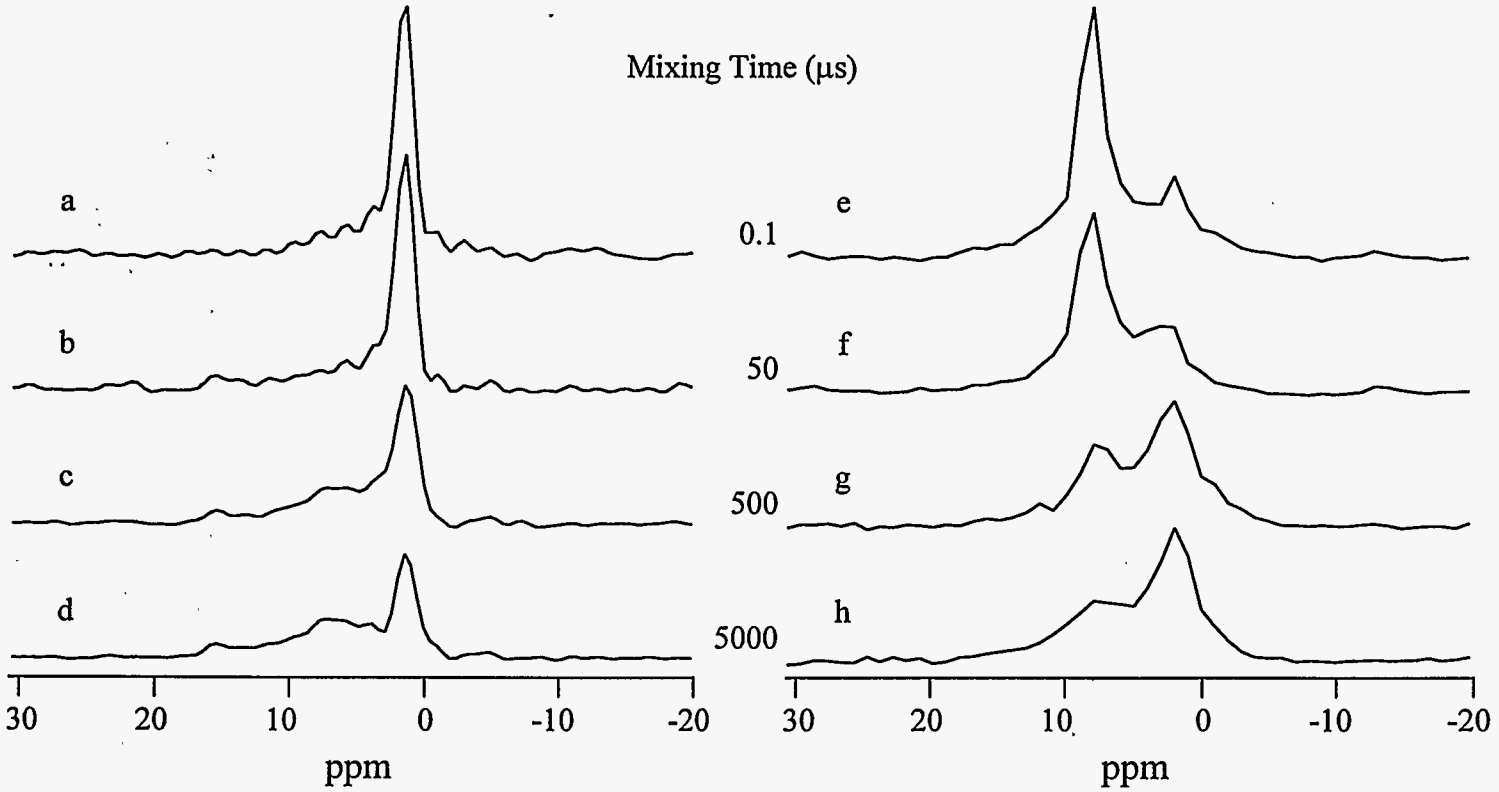

Figure 11.7 Slices cut from the 2D ^{1}H-^{1}H spin-exchange spectra of premium coal 601 shown in Figure 11.6. Slices cut along ω_1 at 1.0 ppm are shown in (a), (b), (c) and (d). Slices cut along ω_2 at 6.9 ppm are shown in (e), (f), (g) and (h). The corresponding mixing times used in the experiments are labeled by the side of each slice.

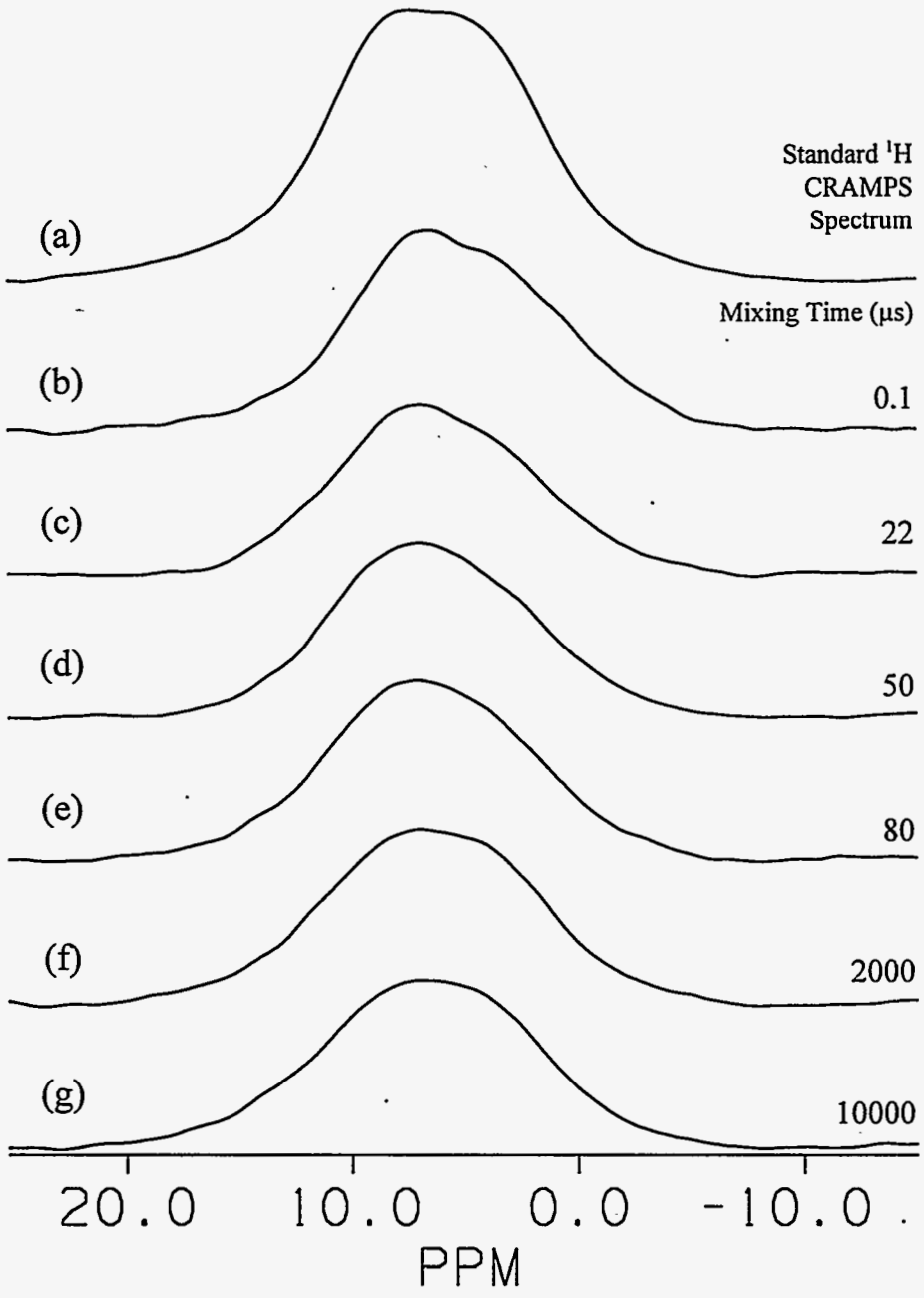

Figure 11.8 ^{1}H CRAMPS spectra of premium coal 501 obtained at 25 ^{0}C in a 1D spin-exchange experiment using the pulse sequence shown in Figure 11.1c. The mixing times were set as (b) 0.1 μs, (c) 22 μs, (d) 50 μs, (e) 80 μs, (f) 2 ms, and (g)10 ms. The dipolar dephasing period was 30 μs. The BR-24 pulse sequence was used with a cycle time of 108 μs and a 90^0 pulse width of 1.25 μs. Each spectrum was acquired with 400 scans and a 3 s recycle delay. The MAS speed was 1.6 kHz. For comparison, a standard ^{1}H CRAMPS spectrum of premium coal 501 obtained at 25 ^{0}C is shown in (a).

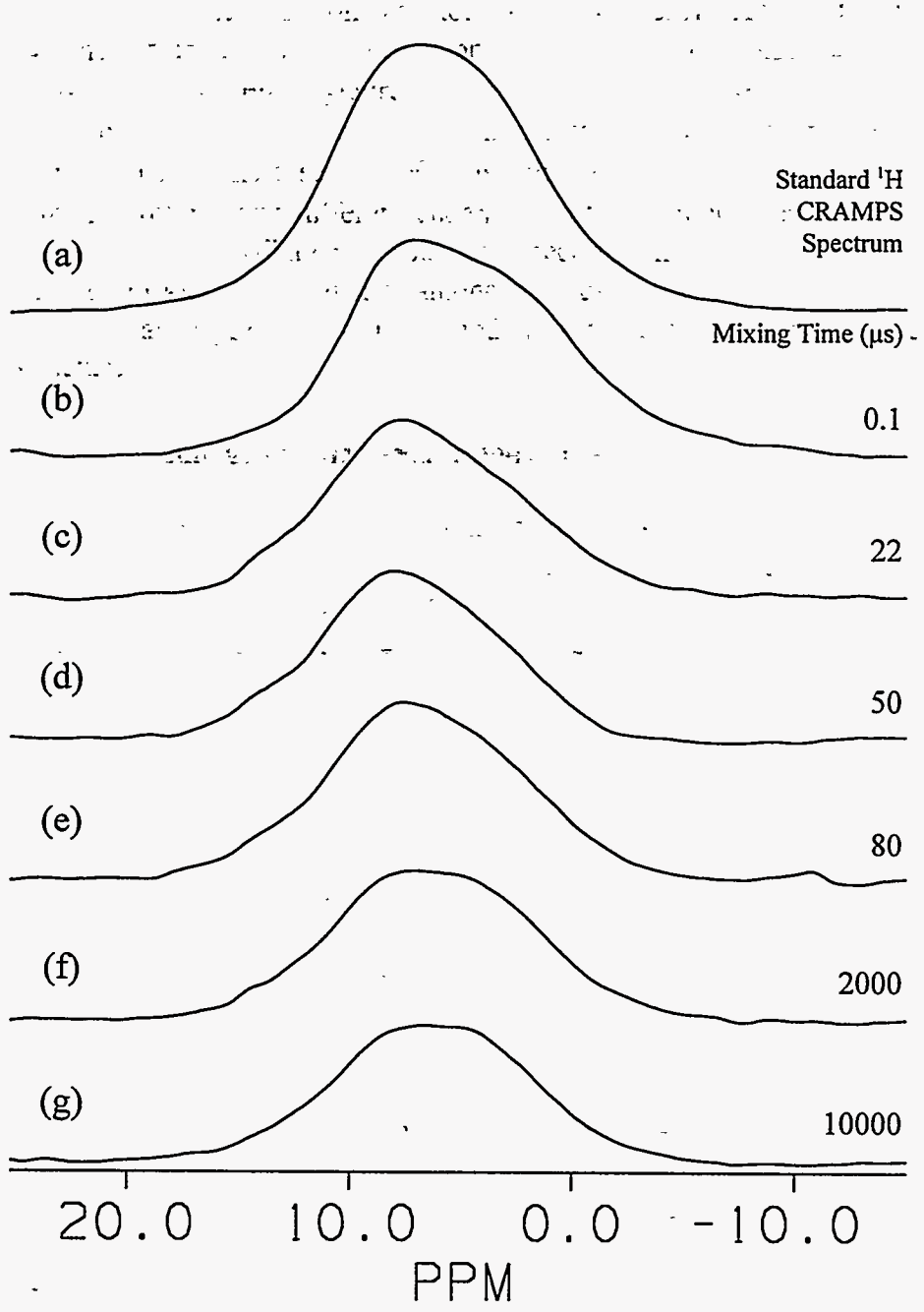

Figure 11.9 ^{1}H CRAMPS spectra of premium coal 501 obtained at 180 ^{0}C in a 1D spin-exchange experiment using the pulse sequence shown in Figure 11.1c. The mixing times were set as (b) 0.1 μs, (c) 22 μs, (d) 50 μs, (e) 80 μs, (f) 2 ms, and (g)10 ms. The dipolar dephasing period was 30 μs. The BR-24 pulse sequence was used with a cycle time of 108 μs and a 90^0 pulse width of 1.25 μs. Each spectrum was acquired with 400 scans and a 3 s recycle delay. The MAS speed was 1.6 kHz. For comparison, a standard ^{1}H CRAMPS spectrum of premium coal 501 obtained at 25 ^{0}C is shown in (a).

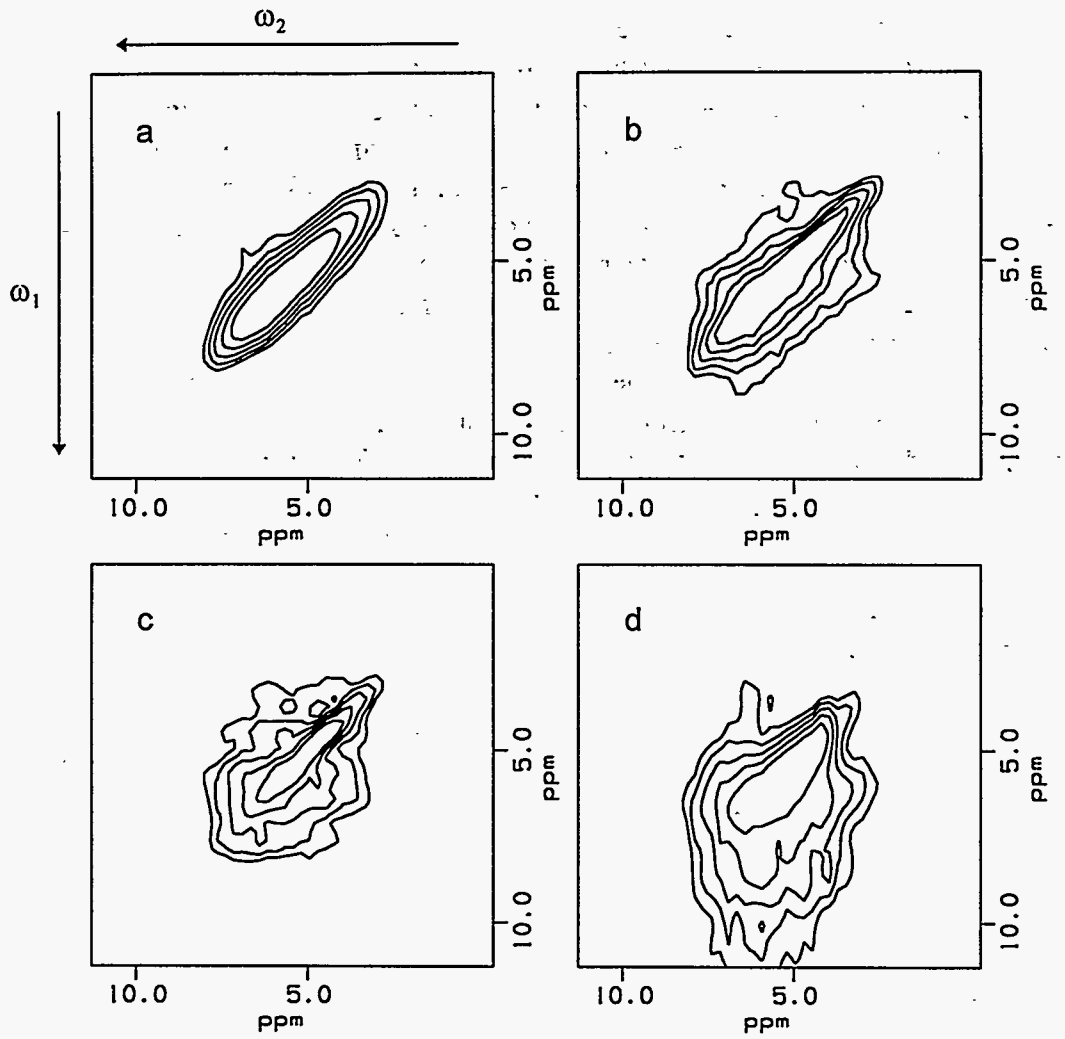

Figure 11.10 Contour plots of the pure absorption 2D ^{1}H-^{1}H spin-exchange spectra of premium coal 501 obtained at 25 ^{0}C with mixing times of (a) 0.1 μs, (b) 50 μs, (c) 500 μs, and (d) 5 ms. The pulse sequence is that shown in Figure 11.2b, with a dephasing period of 30 μs. The increment of the evolution period was one BR-24 cycle, or 108 μs. The original data consisted of 64 256-point BR-24 spectra, each acquired with 400 scans and a 3 s recycle delay. The BR-24 pulse sequence was used with a cycle time of 108 μs and a 90^0 pulse width of 1.2 - 1.3 μs. The MAS speed was 1.6 kHz.

the ω_1 axis at a chemical shift of 1.0 ppm. The decrease of peak intensity at 1.0 ppm in the slice with increasing mixing time reflects the intensity decrease of the diagonal aliphatic peak in the 2D spectrum, due to its spreading along the ω_2 direction or transferring of magnetization to cross peaks with the aromatic peak. Comparing Figure 11.7b with Figure 11.5b, it is very clear that spin-exchange within small aliphatic domains is not appreciable with a mixing time less than 50 μs at 180 ^{0}C, but is significant at 25 ^{0}C. Growth of the cross peak in the aromatic region is also slower at 180 ^{0}C than at 25 ^{0}C, as can be seen by comparing Figures 11.7c and 11.5c.

Figures 11.7e-h show slices cut along the ω_2 axis at a chemical shift of 6.9 ppm. We can see that the slice (Figure 11.7f) corresponding to a mixing time of 50 μs is not dramatically different from that corresponding to a mixing time of 0.1 μs. Again, this implies that highly efficient aliphatic-aromatic spin exchange does not occur at 180 ^{0}C within 50 μs. The growth of cross peaks in the aliphatic region and spreading of the diagonal aromatic peak along the ω_2 axis are clearly seen in the slices obtained with mixing times of 500 μs and 5 ms. The slice corresponding to a mixing time of 5 ms looks very close to the "normal" ^{1}H CRAMPS spectrum of premium coal 601. This again suggests that spin-exchange is close to complete within 5 ms at 180 ^{0}C.

As seen in the discussion above, the new 2D exchange experiment provides many structural and dynamical details of coal, which are not available from other techniques. Various spin-exchange pathways can be differentiated and identified from such studies. The spin-exchange process can be easily monitored semi-quantitatively from the 2D spin-exchange spectral change versus mixing time.

11.4.2 Spin Exchange in Premium Coal 501

The same type of 1D and 2D spin-exchange experiments were also carried out on premium coal 501. Figures 11.8 and 11.9 illustrate stack plots of ^{1}H CRAMPS spectra of premium coal 501 obtained in 1D spin-exchange experiments at 25 ^{0}C and 180 ^{0}C, respectively, with a dipolar-dephasing period of 30 μs.

At 25 ^{0}C, there is only one Gaussian dipolar-dephasing component for either the aliphatic or aromatic protons. Based on the dipolar-dephasing constants measured at 25 ^{0}C, one can estimate that 6% of the signals from aliphatic protons and 10% of the signals from aromatic protons are retained after the 30 μs dipolar-dephasing period. The aliphatic region of the ^{1}H CRAMPS spectrum obtained with a short mixing period should show a depletion of signal intensity relative to the aromatic region. This is clearly seen in Figure 11.8b. A significant change in the spectral line shape can be seen with a mixing time as short as 20 μs, and the shape of the original ^{1}H CRAMPS spectrum returns with a mixing time of 10 ms. This suggests that ^{1}H-^{1}H spin diffusion in premium coal 501 is also very efficient. Similar features can be seen in ^{1}H CRAMPS spectra obtained in a 1D spin-exchange experiment at 180 ^{0}C, as shown in Figure 11.9.

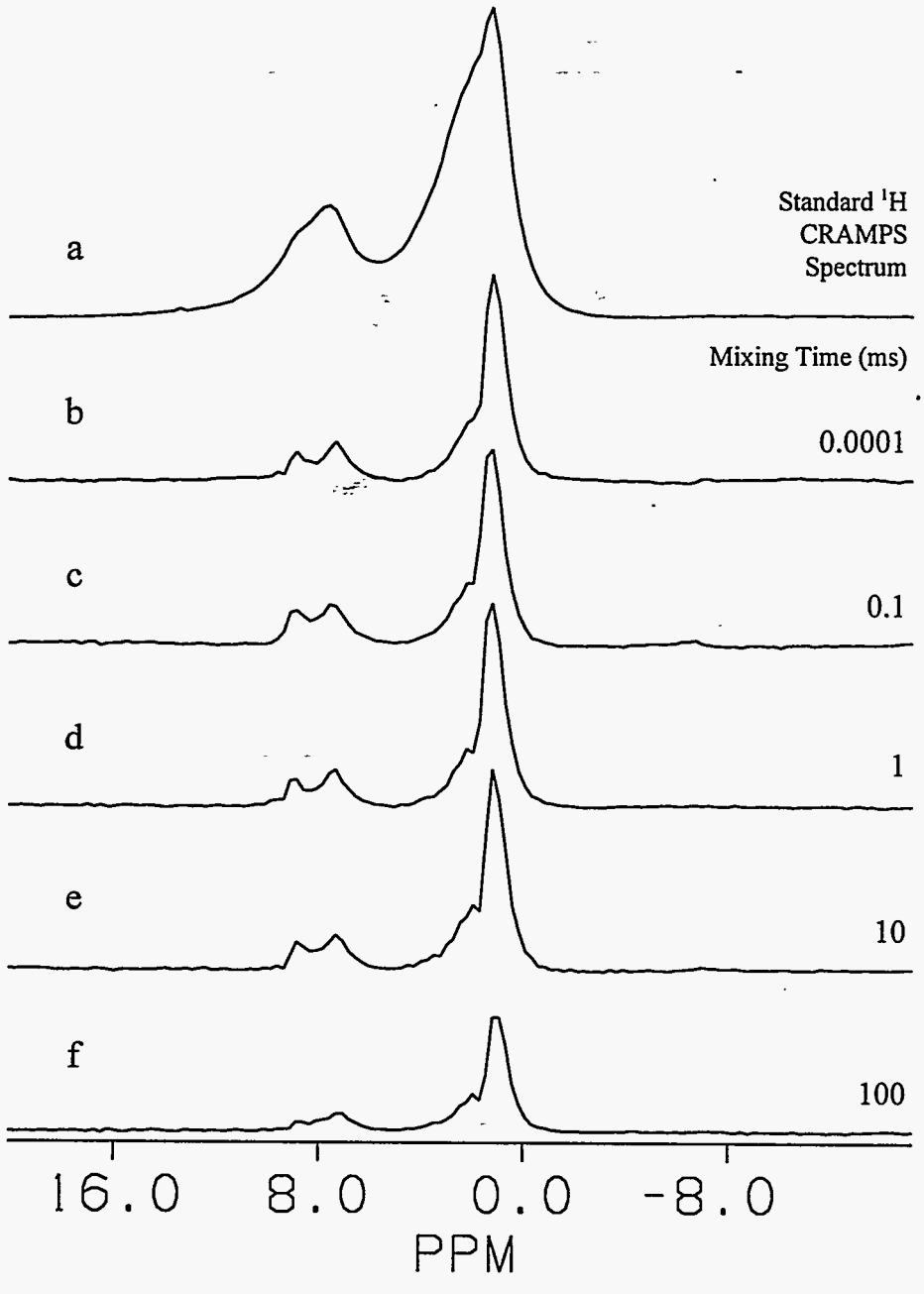

Figure 11.11 ^{1}H CRAMPS spectra of C_5D_5N-saturated premium coal 601 obtained at 25 ^{0}C in a 1D spin-exchange experiment using the pulse sequence shown in Figure 11.1c. The mixing times were set as (b) 0.1 μs, (c) 0.1ms, (d) 1 ms, (e) 10 ms, and (f) 100 ms. The dipolar dephasing period was 200 μs. The BR-24 pulse sequence was used with a cycle time of 108 μs and a 90^0 pulse width of 1.2 - 1.3 μs. Each spectrum was acquired with 500 scans and 3 s recycle delay. The MAS speed was 1.6 kHz. For comparison, a standard ^{1}H CRAMPS spectrum of the same sample obtained at 25 ^{0}C is shown in (a).

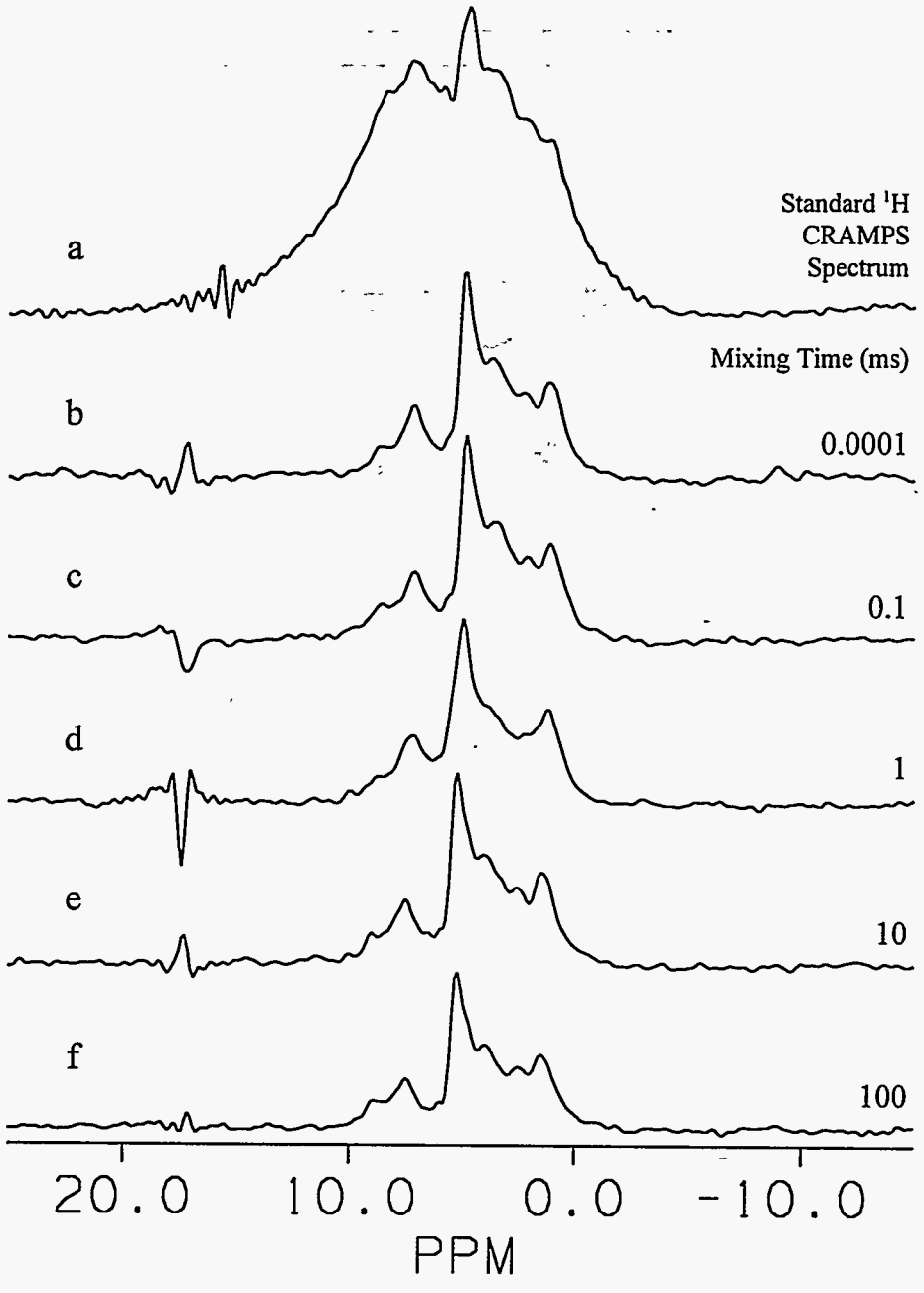

Figure 11.12 ^{1}H CRAMPS spectra of C_5D_5N-saturated premium coal 501 obtained at 25 ^{0}C in a 1D spin-exchange experiment using the pulse sequence shown in Figure 11.1c. The mixing times were set as (b) 0.1 μs, (c) 0.1ms, (d) 1 ms, (e) 10 ms, and (f) 100 ms. The dipolar dephasing period was 200 μs. The BR-24 pulse sequence was used with a cycle time of 108 μs and a 90^0 pulse width of 1.2 - 1.3 μs. Each spectrum was acquired with 1000 scans and 3 s recycle delay. The MAS speed was 1.5 kHz. For comparison, a standard ^{1}H CRAMPS spectrum of the same sample obtained at 25 ^{0}C is shown in (a).

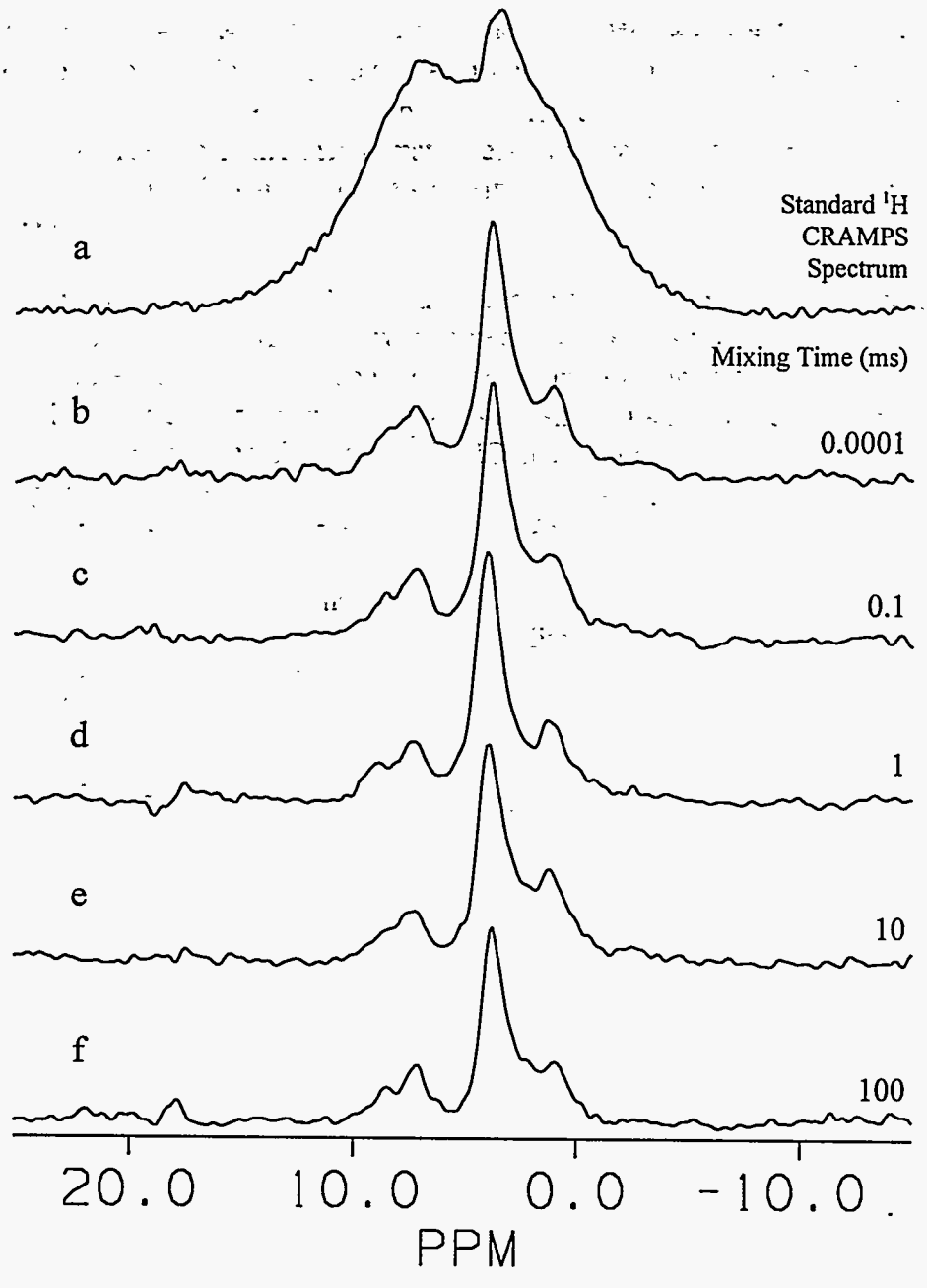

Figure 11.13 ^{1}H CRAMPS spectra of C_5D_5N-saturated premium coal 501 obtained at 90 ^{0}C in a 1D spin-exchange experiment using the pulse sequence shown in Figure 11.1c. The mixing times were set as (b) 0.1 μs, (c) 0.1ms, (d) 1 ms, (e) 10 ms, and (f) 100 ms. The dipolar dephasing period was 200 μs. The BR-24 pulse sequence was used with a cycle time of 108 μs and a 90^0 pulse width of 1.2 - 1.3 μs. Each spectrum was acquired with 1000 scans and 3 s recycle delay. The MAS speed was 1.5 kHz. For comparison, a standard ^{1}H CRAMPS spectrum of the same sample obtained at 90 ^{0}C is shown in (a).

Figure 11.10 illustrates 2D contour plots of 2D spin-exchange spectra of premium coal 501 obtained at 25 ^{0}C with a 30 μs dephasing period and mixing periods of 0.1 μs, 50 μs, 500 μs and 5 ms. From Figure 11.10b, one can clearly see that within a mixing time of 50 μs spin exchange occurs mainly among protons with similar chemical shifts. As the mixing time is increased to 500 μs (Figure 11.10c), various spin-exchange pathways among protons with different chemical shifts and mobilities can be identified. At a mixing time of 5 ms (Figure 11.10d), the spectral density spread out over the 2D spectrum due to further spin-diffusion among various types of protons. Such a spin diffusion pattern may suggest a uniformly random distribution of aliphatic structures and aromatic structures.

11.5 ^{1}H-^{1}H Spin Exchange in C_5D_5N-Saturated Coals

We have previously shown that pyridine-saturation can dramatically change the structure and molecular mobility of coal. In additional to Gaussian dipolar-dephasing component(s) with dipolar-dephasing time constants less than 90 μs, two Lorentzian dipolar-dephasing components with dephasing time constants from 0.13 to 11 ms were identified in C_5D_5N-saturated coal. The nature of the mobile Lorentzian dephasing components are discussed in detail elsewhere.

Previous dipolar-dephasing experiments strongly suggest that a significant fraction of the Lorentzian dephasing components correspond to protons in small molecules that undergo rapid rotational motion in large pores created by cleavage of hydrogen bonding bridges in the macromolecular network. A study of spin-diffusion between mobile Lorentzian components and rigid Gaussian dephasing components should provide more direct information on the spatial distribution of protons with different mobilities. It would also be interesting to see if there is any significant spin exchange among mobile protons with different chemical shifts, which are well resolved in ^{1}H CRAMPS spectra of mobile protons showing Lorentzian dephasing behaviors. Such spin-exchange processes would be mainly contributed from intramolecular dipolar couplings among protons in different structural moieties, because Lorentzian dephasing components are very mobile. The degree of substitution of aromatic rings could then be estimated from the ratio of the intensity of the cross peak between aliphatic and aromatic peaks to the intensity of the diagonal aromatic peak.

11.5.1 Spin Exchange between Lorentzian Dephasing Components and Gaussian Dephasing Components

As large difference of dephasing time constants exists between Lorentzian and Gaussian dipolar-dephasing components, a dipolar-dephasing period can be used to select mobile Lorentzian dephasing component in a spin-exchange experiment. In this work, a dipolar-dephasing period of 200 μs was used in all the spin-exchange experiments discussed below.

Figure 11.11 shows a stack plot of ^{1}H CRAMPS spectra of C_5D_5N-saturated premium coal 601 obtained in 1D spin-exchange experiments at 25 ^{0}C with mixing times from 0.1 μs to 100 ms. If there is significant spin-exchange between Lorentzian and Gaussian dephasing components, the resolution of highly resolved ^{1}H CRAMPS spectra of mobile protons would degrade as the mixing time increases. With a sufficiently long mixing period, the original ^{1}H CRAMPS spectrum of C_5D_5N-saturated coal (Figure 11.11a) should be at least partially restored. However, Figure 11.11 clearly show that there is no significant change in the shape and relative intensity of each peak in the ^{1}H CRAMPS spectrum obtained with a mixing time up to 100 ms. This proves that there is no significant spin-exchange between the Lorentzian dephasing components and the Gaussian dephasing components within 100 ms. A decrease in the total integrated intensity of the ^{1}H CRAMPS spectrum obtained with a mixing time of 100 ms (Figure 11.11f) can be seen. This is due to the effect of spin-lattice relaxation (T_1) during the mixing period[12]. In fact, the ^{1}H spin-lattice relaxation time places a limit on the largest mixing time possible for a spin-exchange experiment.

Figures 11.12 and 11.13 illustrate stack plots of ^{1}H CRAMPS spectra of C_5D_5N-saturated premium coal 501 obtained in 1D spin-exchange experiments with mixing times from 0.1 μs to 100 ms at temperatures of 25 ^{0}C and 90 ^{0}C, respectively. There is also no significant change of shape and relative intensity of each peak in ^{1}H CRAMPS spectra obtained either at 25 ^{0}C or 90 ^{0}C, as the mixing time is varied up to 100 ms. This demonstrates again that there is no significant spin-exchange between protons with Lorentzian dephasing characteristic and protons showing Gaussian dephasing behavior in C_5D_5N-saturated coal.

The above results can be used to estimate a lower limit on the size of domains (L_L) of Lorentzian dephasing components. As the spin-diffusion between Lorentzian and Gaussian dephasing components is not significant with mixing time τ_m at least up to 100 ms, L_L must be larger than the effective spin-diffusion distance of protons showing Lorentzian dephasing behavior, or:

$$L_L > \sqrt{6 D_L \tau_m} \qquad (11.16)$$

where τ_m = 100 ms, and D_L is the spin-diffusion coefficient of a Lorentzian dephasing component. For Lorentzian dephasing components, D_L can be estimated from the dephasing constants T_{dd} according to equation (11.13). Plugging equation (11.13) into expression (11.16), we have

$$\frac{L_L}{\sqrt{\langle d^2 \rangle}} > \sqrt[4]{\beta}\sqrt{\frac{\tau_m}{T_{dd}}} \qquad (11.17)$$

where $<d^2>$ is the mean square distance between the nearest protons in Lorentzian dephasing components.

As we don't know the exact molecular structure of Lorentzian dephasing components, an estimation on $<d^2>$ is difficult. Nevertheless, the ratio $L_L/\sqrt{<d^2>}$ can give us an idea how far mobile protons are away from rigid protons in the macromolecular structure of coal in terms of $\sqrt{<d^2>}$. For fast Lorentzian dephasing components, we can estimate $L_L/\sqrt{<d^2>}$ to be greater than 40, using T_{dd} = 0.2 ms and β =10. For slow Lorentzian dephasing components, $L_L/\sqrt{<d^2>}$ is estimated to be greater than 6, using T_{dd} = 10 ms and β = 10. As the τ_m used in this experiment is limited by T_1, underestimation of $L_L/\sqrt{<d^2>}$ should be much more severe for slow dephasing Lorentzian components than that for fast Lorentzian dephasing components. From dipolar-dephasing experiments, we know that slow Lorentzian dephasing components should be located in larger pores than are fast Lorentzian dephasing components. Therefore, the ratio, $L_L/\sqrt{<d^2>}$, for slow Lorentzian dephasing components should be at least as large as that for fast dephasing components.

As discussed in Section 11.2.3, a rough estimation of $<d^2>$ is about 3 Å. That gives a minimum domain size of Lorentzian dephasing components of at least 120 Å. The number average molecular weight of extractable small molecules in coal has been reported to be about 600[13]. This means that the average number of carbons in a small molecule is around 40 - 50. That gives us a picture of small molecules packed in large pores of macromolecular matrix. This kind of rough estimation is compatible with our view of the structural and dynamical changes in coal induced by pyridine saturation.

11.5.2 Spin Exchange among Mobile Protons with Lorentzian Dephasing Characteristics

We showed in the last section that there is no appreciable ^1H-^1H spin-exchange between Lorentzian dephasing components and Gaussian dephasing components within 100 ms in C_5D_5N-saturated coals. The study of spin exchange processes among mobile protons of Lorentzian dephasing components is thus simplified, since exchange pathways between Lorentzian dephasing components and Gaussian components are excluded. As the ^1H CRAMPS spectra of mobile protons show several well resolved peaks, the newly designed 2D spin-exchange pulse sequence is well suited for studying spin-exchange process among mobile protons of different chemical shifts.

Figures 11.14 and 11.15 show contour plots of 2D spin-exchange spectra of C_5D_5N-saturated premium coal 601 obtained at 25 ^{0}C with mixing times of 10 ms and 100 ms. A dipolar dephasing period of 200 μs was used to filter out signals from rigid Gaussian dephasing components. Before we get into the details of these spectra, we make some comments on the interpretation of some spectral features in a contour plot of a 2D spin-exchange spectrum.

In a 2D experiment, data points collected in the t_1 dimension are usually limited by the available experimental time and may be severely truncated. Therefore, resolution in the

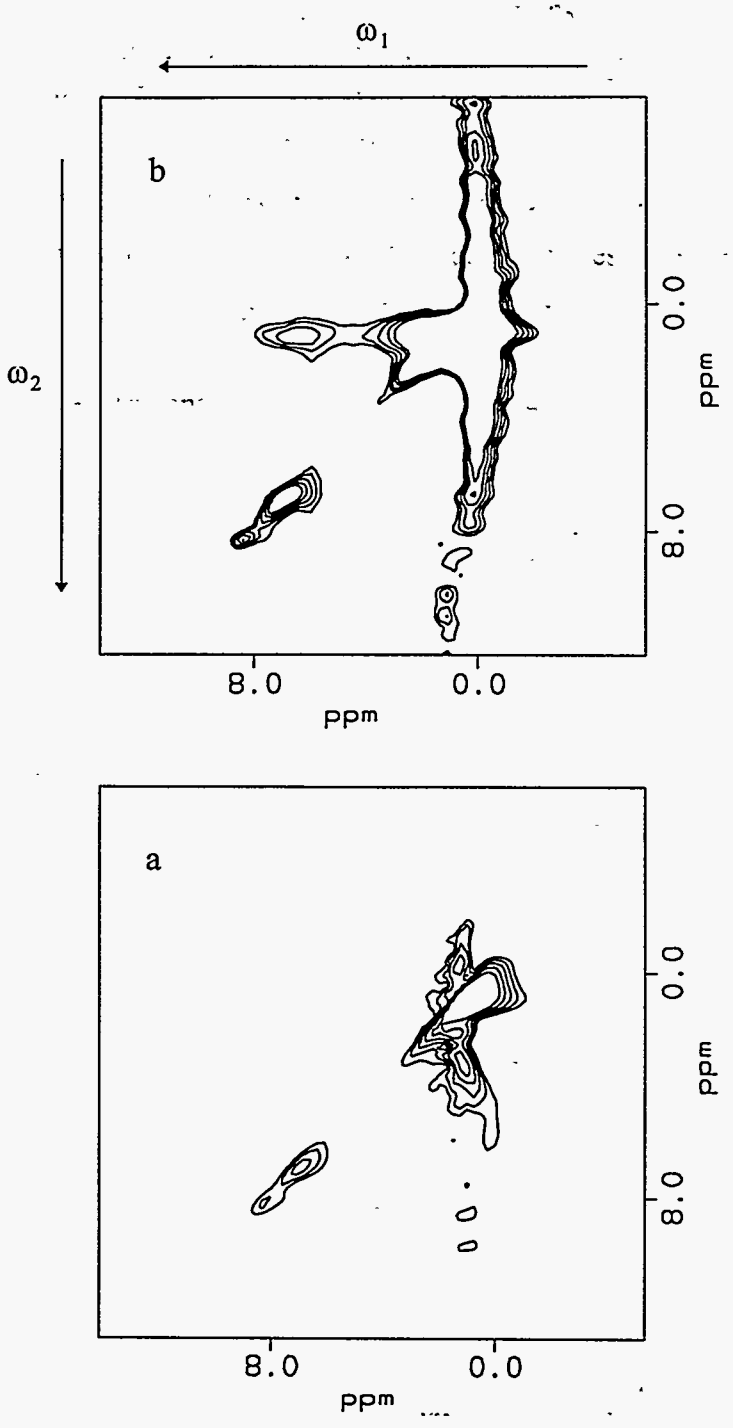

Figure 11.14 Contour plots of pure absorption 2D ^{1}H-^{1}H spin-exchange spectra of C_5D_5N-saturated premium coal 601 obtained at 25 ^{0}C with a mixing time of (a) 10 ms and (b) 100ms. The pulse sequence is that shown in Figure 11.2b, with a dephasing period of 200 μs. The increment of the evolution period was one BR-24 cycle, or 108 μs. The original data consisted of 128 256-point BR-24 spectra, each acquired with 200 scans and a 3 s recycle delay. The BR-24 pulse sequence was used with a cycle time of 108 μs and a 90^0 pulse width of 1.2 - 1.3 μs. The MAS speed was 1.6 kHz.

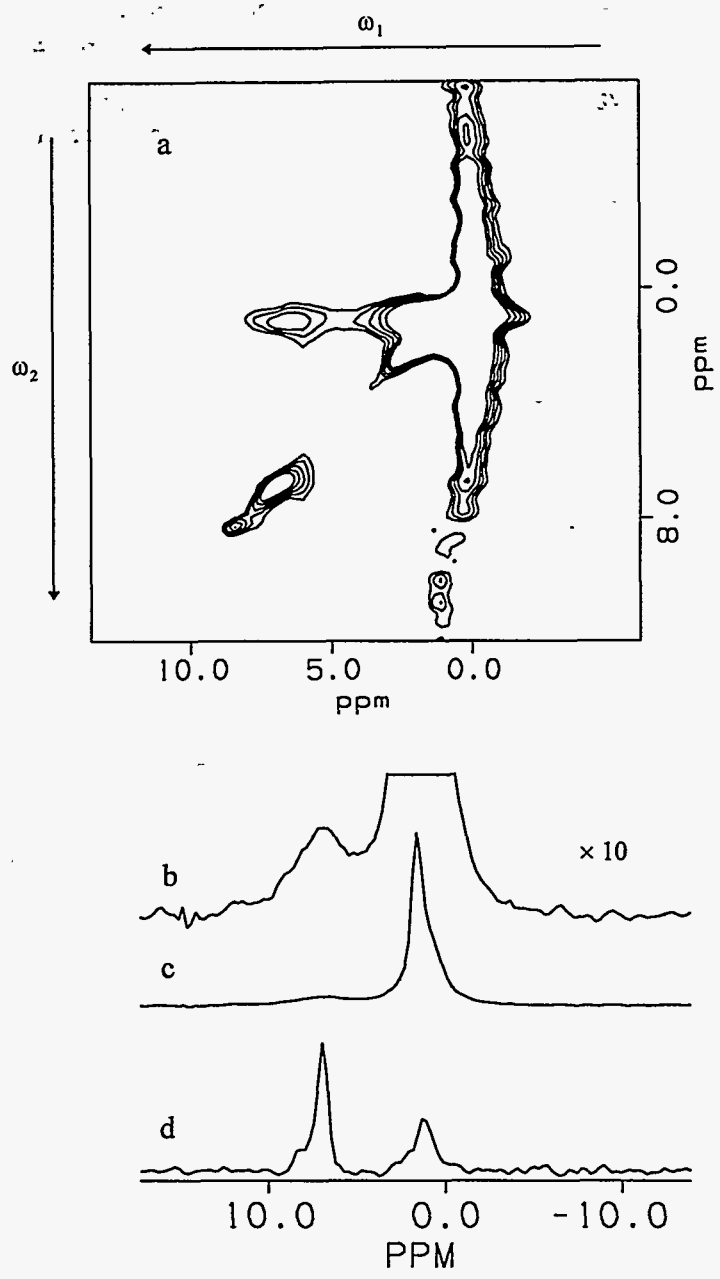

Figure 11.15 (a) Contour plot of the pure absorption 2D ^1H-^1H spin-exchange spectrum of C_5D_5N-saturated premium coal 601 obtained at 25 ^0C with a mixing time of 100 ms. The pulse sequence is that shown in Figure 11.2b, with a dephasing period of 200 μs. The increment of the evolution period was one BR-24 cycle, or 108 μs. The original data consisted of 128 256-point BR-24 spectra, each acquired with 200 scans and a 3 s recycle delay. The BR-24 pulse sequence was used with a cycle time of 108 μs and a 90^0 pulse width of 1.2 - 1.3 μs. The MAS speed was 1.6 kHz. (c) Slice cut along ω_2 at 1.0 ppm. (b) A vertically magnified (10 times) view of (c). (d) Slice cut along ω_1 at 6.9 ppm.

ω_1 dimension is usually worse than that in the ω_2 dimension, and severe distortions of the baseline around a strong and narrow peak in the ω_1 dimension may be observed. In this case small peaks on ω_1 dimension may be difficult to identify. This is the case for the strong diagonal aliphatic peak at 1.0 ppm in Figures 11.14 and 11.15. Cross peaks between this aliphatic peak and the aromatic peak are clearer in the upper right corners of Figures 11.15 and 11.17 than in the lower left corners, because of the distortions along the ω_1 dimension.

As the aliphatic peak of C_5D_5N-saturated coal 601 at 1.0 ppm is much stronger than other peaks in the ^1H CRAMPS spectrum, especially after a substantial dipolar-dephasing period, we have to set a very low contour level in the contour plot in order to present the 2D spin exchange spectra properly. As a result, small distortions around the bottom of the strong aliphatic peak can show up in the 2D spectrum. That is the origin of much of the off diagonal spectral intensity in Figure 11.14. It is usually easy to distinguish a real cross peak from small spectral distortions by examining slices cut from the 2D spectrum.

Another thing worth mentioning here is that Lorentzian and Gaussian peaks in a pure absorption-mode 2D spectrum show distinctively different contour shapes in a 2D contour plot. A Gaussian peak shows circular contours, while a Lorentzian peak shows a star shaped contour, as shown in Figure 11.16. The strong aliphatic peak at 1.0 ppm in the 2D spin-exchange spectra (Figures 11.14 and 11.17) of C_5D_5N-saturated coal is close to Lorentzian in shape. At the bottom of the aliphatic peak, the contour extends along the ω_1 and ω_2 axes. This kind of feature can be seen in Figures 11.14, 11.15 and 11.17.

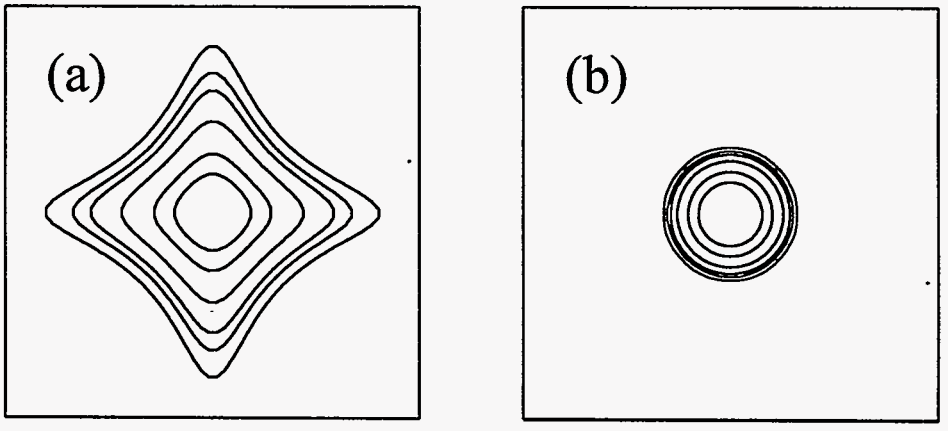

Figure 11.16 Contour plots of (a) a 2D Lorentzian peak and (b) a 2D Gaussian peak.

We now return to analyze the 25 ^0C 2D spin-exchange spectrum of C_5D_5N-saturated coal 601 shown in Figure 11.14. One can clearly see that there is no significant build-up of cross peaks with a mixing time of 10 ms (Figure 11.14a). This fact is consistent with results of the dipolar-dephasing experiments obtained previously in this project. If spin exchange among mobile protons were very efficient within 10 ms, we would not have

been able to identify two Lorentzian components with distinctly different dipolar-dephasing constants. These results also suggest that intramolecular dipolar coupling between structurally different types of protons (aliphatic and aromatic) is weak. This implies that the Lorentzian dephasing components undergo very rapid rotational motion, which effectively averages intramolecular dipolar interactions.

With a mixing time of 100 ms (Figure 11.14b), small cross peaks between the aliphatic peak and the aromatic peak are clearly identified. As we have found that there is no detectable spin diffusion between the Lorentzian dephasing components and the Gaussian dephasing components within 100 ms, the cross peak should be mainly due to the intramolecular dipolar couplings between protons attached to aromatic rings and protons in aliphatic substituents of aromatic structures of Lorentzian dephasing components. Therefore, the intensity ratio of the cross peak to the diagonal aromatic peak provides a measure of the degree of substitution of aromatic ring systems of Lorentzian dephasing components. The intensity ratio of the cross peak to the diagonal aliphatic peak reflects the ratio of protons in aliphatic substituents on aromatic structures to protons in aliphatic molecules.

The relative intensity of the cross peak to diagonal aliphatic and aromatic peaks can be clearly seen in slices cut parallel to the ω_1 and ω_2 axes. Figures 11.15c shows a slice cut parallel to the ω_1 axis at 1.0 ppm. The cross peak in the aromatic region is much smaller than the diagonal aliphatic peak at 1.0 ppm. By magnifying the vertical scale of the slice by 10 times, the cross peak is easily recognizable in Figure 11.15b. Figure 11.15d shows a slice cut along ω_2 at 6.9 ppm. The intensity of the cross peak shown in the aliphatic region is close to that of the diagonal aromatic peak at 6.9 ppm. This result suggests that most of the mobile aliphatic protons with Lorentzian dephasing characteristics are in structures consisting of only aliphatic moieties. However, the mobile aromatic protons showing Lorentzian dephasing behaviors are likely to be distributed in aromatic structures with substantial aliphatic substituents. This is consistent with the recent studies on the molecular structure of pyridine extracts of coal[37,38]. Our dipolar-dephasing results strongly suggest that most of the fast Lorentzian dephasing aromatic protons are associated with mobile macromolecular chains in coal. The spin exchange results imply that a significant fraction of the flexible aliphatic side chains present are attached to the mobile aromatic main chains of macromolecular structures in coal, which undergo rapid segmental motion.

Figure 11.17a shows a contour plot of 2D spin-exchange spectra of the same sample at a higher temperature, 90 ^{0}C, with a mixing time of 100 ms. Cross peaks between aliphatic and aromatic protons can still be identified. Although the aromatic cross peak is hardly recognizable at a quick glance of the slice cut parallel to ω_1 at 1.0 ppm (Figure 11.17c), the cross peak is clearly identified in a vertically magnified view of the same slice (Figure 11.17b). Comparing Figures 11.15c, 11.17c, one can see that the intensity ratio of cross peak to diagonal aliphatic peak at 90 ^{0}C is lower than the corresponding one at 25 ^{0}C. These observations are consistent with VT dipolar dephasing studies on C_5D_5N-

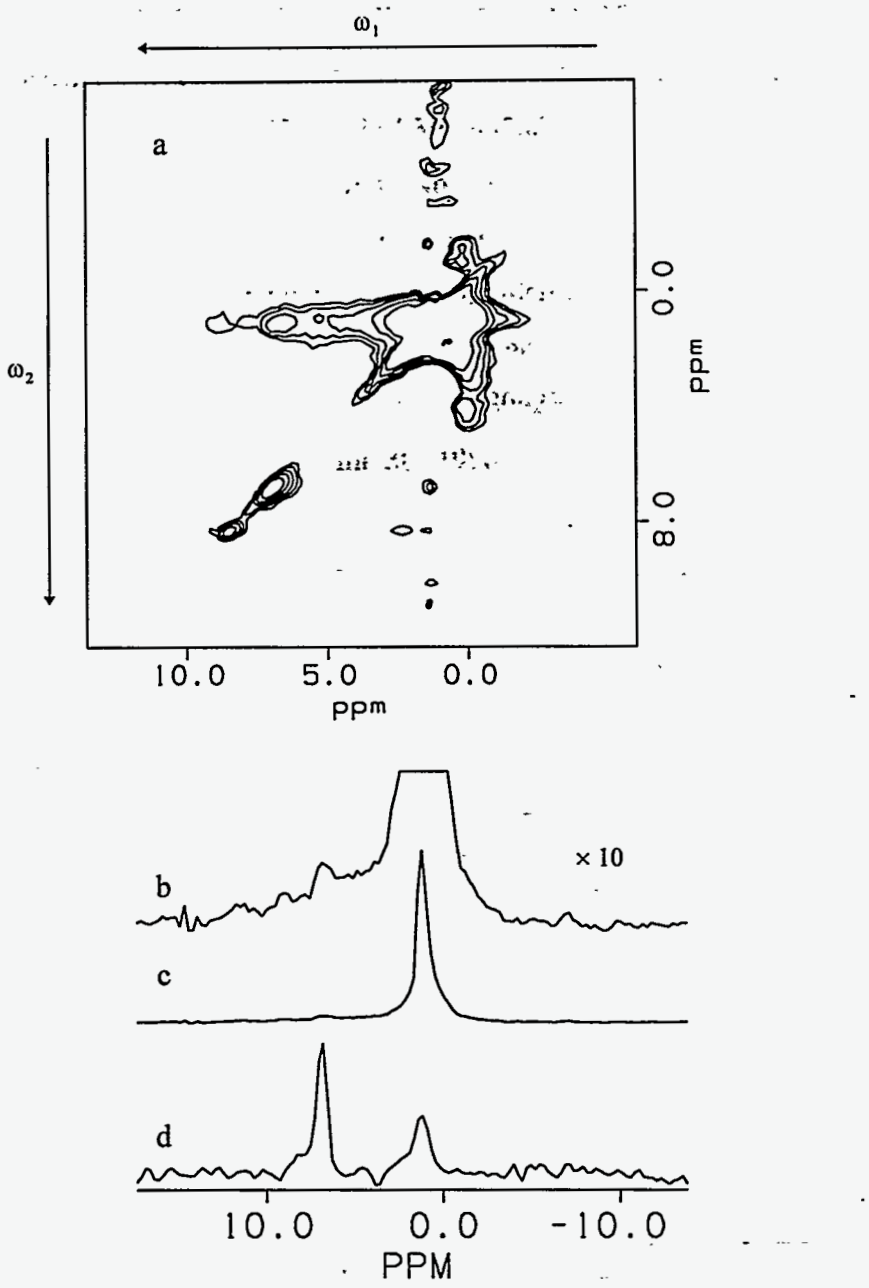

Figure 11.17 (a) Contour plot of the pure absorption 2D ^{1}H-^{1}H spin-exchange spectrum of C_5D_5N-saturated premium coal 601 obtained at 90 ^{0}C with a mixing time of 100 ms. The pulse sequence is that shown in Figure 11.2b, with a dephasing period of 200 μs. The increment of the evolution period was one BR-24 cycle, or 108 μs. The original data consisted of 128 256-point BR-24 spectra, each acquired with 200 scans and a 3 s recycle delay. The BR-24 pulse sequence was used with a cycle time of 108 μs and a 90^0 pulse width of 1.2 - 1.3 μs. The MAS speed was 1.6 kHz. (c) Slice cut along ω_2 at 1.0 ppm. (b) A vertically magnified (10 times) view of (c). (d) Slice cut along ω_1 at 6.9 ppm.

saturated premium coal 601 carried out earlier in this project. When the temperature is increased from 25 ^{0}C to 90 ^{0}C, the Lorentzian dephasing components (the sum of both fast and slow dephasing components) of aliphatic protons are increased from 35% to 46%, while Lorentzian dephasing components of aromatic protons are increased from 14% to 19%. The 2D spin exchange results suggest that the increase of mobile Lorentzian dephasing aliphatic protons at 90 ^{0}C is mainly due to structures with low aromaticity. However, the cross-peak intensity in the slice cut parallel to ω_1 at 6.9 ppm is close to the intensity of the diagonal aromatic peak. The intensity ratio of the cross peak to the diagonal aromatic peak at 25 ^{0}C is very close to the ratio at 90 ^{0}C, as shown in Figures 11.15d and 11.17d. This result implies that the degree of substitution of aromatic structures of Lorentzian dephasing components at 25 ^{0}C is very close to that at 90 ^{0}C.

The 2D spin-exchange studies presented in this chapter clearly demonstrate the power and potential of the new 2D spin-exchange pulse sequence for elucidating structural and dynamical details of very complicated heterogeneous systems.

References

1. Cheng, T. P. P.; Gerstein, B. C. *J. Appl. Phys.*, **1981**, 52, 5517.
2. Cheng, T. P. P.; Gerstein, B. C.; Rayan, L. M.; Taylor, R. E.; Dybowski, D. R. *J. Chem. Phys.*, **1980**, 73, 6059.
3. Packer, K. J.; Pope, J. M.; Yeung, R. R.; Cudby, M. E. A. *J. Polym. Sci. Polym. Phys. Ed.*, **1984**, 22, 589.
4. Havens, J. R.; VanderHart, D. L. *Macromolecules*, **1985**, 18, 1663.
5. Caravitti, P.; Neuenschwandler, P.; Ernst, R. R. . *Macromolecules*, **1986**, 19, 1895.
6. Caravitti, P.; Neuenschwandler, P.; Ernst, R. R. . *Macromolecules*, **1986**, 18, 1663.
7. Colquhoun I. C.; Packer, K. *Brit. Polym. J.*, **1987**, 19, 151.
8. Clauss J.; Schmidt-Rohr K.; Spiess H. W. *Acta Polymer*, **1993**, 44, 1.
9. Tekely, P.; Canet, D.; Delpuech, J. J. *Mol. Phys.*, **1989**, 67, 81.
10. Belfiore, L. A.; Lutz, T. J.; Cheng, C.; Bronnimann, C. E. *J. Polym. Sci. Polym. Phys.*, **1990**, 28, 1261.
11. Demco, D. E.; Johansson, A.; Tegenfeldt, J. *Solid State Nucl. Magn. Reson.*, **1995**, 4, 13.
12. Schmidt-Rohr K.; Spiess H. W. *Multidimensional Solid-State NMR and Polymers*, **1994**, Academic Press, London.
13. Derbyshire, F.; Marzec, A.; Schulten, H. -R.; Wilson, M. A.; Davis, A.; Tekely, P.; Delpuech, J. -J.; Jurkiwicz, A.; Bronnimann, C. E.; Wind, R. A.; Maciel, G. E.; Narayan, R.; Bartle, K.; Snape, C. *Fuel*, **1989**, 68, 1091.

14. Barton, W. A.; Lynch, L. J.; Webster, D. S.; Simms, G. In *Magnetic Resonance of Carbonaceous Solids;* Botto, R. E.; Sanada, Y., Eds.; Advances in Chemistry 229; American Chemical Society, Washington, DC, **1993**, p.175.

15. Bloembergen, N. *Physica (Utrecht)*, **1949**, 15, 386.

16. Zhang, S.; Meier, B. H.; Ernst, R. R. *Phys. Rev. Lett*, **1992**, 69, 2149.

17. Crank, J. *Mathematics of Diffusion*, **1956**, Clarendon Press, Oxford.

18. Veeman, W. S.; Maas, W. E. J. R. *NMR Basic Principles and Progress*, 1994, 32, 127.

19. Henrichs, P. M.; Tribone, J; Massa, D. J.; Hewitt, J. M. *Macromolecules*, **1988**, 21, 1282.

20. Cheng, T. T. P *Phys. Rev.*, **1981**, B23, 1404.

21. Goldman, M. *Spin Temperature and Nuclear Magnetic Resonance in Solids*, **1970**, Clarendon Press, Oxford.

22. Gerstein, B. C.; Dybowski, C. *Transient Techniques in NMR of Solids*, **1985**, Academic, New York.

23. Berkowitz, N. in *An Introduction to Coal Technology*, 2nd Ed.; **1994**, Academic Press, San Diego.

24. Edzes, H. T.; Samulski, E. T. *J. Magn. Reson.*, **1978**, 31, 207.

25. Bodenhausen, G.; Freeman, R.; Morris, G. A. *J. Magn. Reson.*, **1976**, 23, 171.

26. Caravatti, P.; Bodenhaussen, G.; Ernst, R. R. *J. Magn. Reson.*, **1983**, 55, 88.

27. Nakai, T.; McDowell, C. A. *J. Magn. Reson.*, **1990**, 90, 426.

28. Caravatti, P.; Levitt, M. H.; Ernst, R. R. *J. Magn. Reson.*, **1986**, 68, 323.

29. Schmidt-Rohr, K.; Clauss, J.; Blumich, B.; Spiess, H. W. *Magn. Reson in Chem.*, **1990**, 28, 3.

30. Goldman, M.; Shen, L. *Phys. Rev.* **1966**, 144, 321.

31. Bronnimann, C. E.; Zeigler, R. C.; Maciel, G. E. *J. Am. Chem. Soc.*, **1988**, 110, 2023.

32. Ridenour, C. R. *Ph.D. Dissertation*, Colorado State University, **1992**.

33. Ernst, R. R.; Bodenhausen, G.; Wokaun, A. *Principles of Nuclear Magnetic Resonance in One and Two Dimensions*, **1987**, Clarendon Press, Oxford.

34. Speiss, H. W. *Annu. Rev. Mater. Sci.*, **1991**, 21, 131.

35. Redfield, A.G.; Kunz, S.D. *J. Magn. Reson.* **1975**, 19, 250.

36. Maciel, G. E.; Bronnimann, C. E.; Hawkins, B. L. *In Advances in Magnetic Resonance: The Waugh Symposium;* Warren, W. S., Ed.; Academic: San Diego, CA, 1990; Vol. 14, p.125.

37. Stefanova, M.; Simoneit, B. R. T.; Stojanova, G.; Nosyrev, I. E.; Goranova, M. *Fuel*, **1995**, 74, 768.

38. Stefanova, M.; Simoneit, B. R. T.; Stojanova, G.; Nosyrev, I. E.; Goranova, M. *Energy Fuel*, **1993**, 7, 734.